

THE DIAMOND POTENTIAL OF THE TUWAWI KIMBERLITE  
(BAFFIN ISLAND, NUNAVUT).

by  
JODI CROSS

A THESIS SUBMITTED IN PARTIAL FULFILLMENT OF  
THE REQUIREMENTS FOR THE DEGREE OF  
BACHELOR OF SCIENCE (HONOURS)

in  
  
THE FACULTY OF SCIENCE  
(Geological Sciences)

This thesis conforms to the required standard

.....  
Supervisor

THE UNIVERSITY OF BRITISH COLUMBIA  
(Vancouver)

MARCH 2009

© Jodi Cross, 2009

## ABSTRACT

---

Ten samples of kimberlite and associated mantle xenoliths were studied to constrain the diamond potential of the Tuwawi kimberlite of Baffin Island, Nunavut. The Tuwawi kimberlite, one in a cluster of 3 kimberlites, is located at the northwestern end of Baffin Island on the Brodeur Peninsula. Baffin Island is underlain by Archean crust of the Rae craton with Paleoproterozoic reworking, and is known to contain several kimberlites, possibly, one at least, of Cretaceous age. These include the Freightrain and Cargo kimberlites.

Petrographic analyses established that both hypabyssal and volcanoclastic kimberlitic types are present among the four kimberlite samples. Hypabyssal kimberlite is the predominant type in Tuwawi, consisting of olivine macrocrysts set in a carbonate-serpentine groundmass with olivine microphenocrysts, phlogopite and spinel. Volcanoclastic kimberlite is characterized by the presence of 1) irregularly-shaped juvenile lapilli; 2) two semi-intermixed dark cryptocrystalline matrix materials; 3) olivine grains with a restricted size distribution and angular shapes. These features suggest mild sorting of the kimberlite, a possible incorporation of mud to the matrix, an epiclastic origin and formation in the crater facies.

Petrographic analyses established that the six mantle xenolith samples include two garnet lherzolites, a spinel and a garnet-spinel harzburgites, a dunite, and a clinopyroxenite. Both coarse and deformed (porphyroclastic and mosaic-porphyroclastic) textures are present within the peridotite xenoliths. Garnet is present in all but one sample, whereas spinel occurs only in coarse peridotites. Electron microprobe geochemical analyses of the mantle xenoliths provided important information regarding the equilibrium compositions of the major minerals present: olivine, orthopyroxene, clinopyroxene, garnet, and spinel. All minerals, except spinel, show chemical homogeneity between and within grains. Cr-diopside from deformed xenoliths shows higher  $\text{TiO}_2$  (0.16 wt%) content than in coarse peridotites. All

garnets present are pyropes ( $\text{Mg}_{81-84}$ ), and spinels are magnesiochromites showing strong chemical heterogeneity. This is controlled by random intra-grain compositional changes in FeO (from 12 to 16 wt%), MgO,  $\text{Al}_2\text{O}_3$  and  $\text{Cr}_2\text{O}_3$  (from 43 to 57 wt% ). Olivine and orthopyroxene in all xenoliths are very magnesian ( $\text{Fo}_{91-92}$  and  $\text{En}_{92-93}$ ), slightly more so in coarse peridotites.

Pressures and temperatures of mineral equilibria for the mantle xenoliths were estimated using various two-pyroxenes, garnet-pyroxene, olivine-garnet, and olivine-spinel geothermobarometers. Deformed garnet lherzolite and garnet clinopyroxenite were formed at 1103-1209°C and 53.8–60 kb. Deformed peridotites are equilibrated at higher temperatures and pressures than coarse peridotites. Garnet peridotites and pyroxenites show higher temperatures than spinel peridotites. These patterns match the commonly observed mantle lithological columns below cratons. In comparison to temperature and pressure data from kimberlites of Somerset Island, xenoliths from Tuwawi plot farther into the diamond stability field and at a lower geothermal gradient ( $\sim 42 \text{ mW/m}^2$ ). The majority of mantle xenoliths from Cretaceous Somerset Island kimberlites plot in the graphite stability field along a geotherm of  $\sim 44 \text{ mW/m}^2$ .

Several factors were identified that give a positive outlook on the diamond potential of the Tuwawi kimberlite. These factors include 1) a preservation of the crater facies kimberlite, and 2) kimberlite sampling of the deep diamondiferous mantle. The diamond potential is reduced by the estimated  $42 \text{ mW/m}^2$  geothermal gradient that is hotter than the desired low geotherm for Archean cratons. In addition, a relatively narrow “diamond window” (i.e. the range of temperatures where diamond is stable in the asthenosphere), 1050-1100 °C, lowers the diamond potential of the Tuwawi kimberlite.

## TABLE OF CONTENTS

---

Title Page.....	i
Abstract.....	ii
Table of Contents.....	iv
List of Figures.....	vi
List of Tables.....	vii
List of Appendices.....	vi
Acknowledgements.....	ix
1) Introduction	
1.1. Purpose.....	1
1.2. Location.....	1
1.3. Previous Work.....	4
2) Geology	
2.1. Tectonic Setting.....	5
2.2. Geological Setting	
2.2.1. Regional Geology.....	7
2.2.2. Local Geology.....	8
3) Petrography of the Tuwawi Kimberlite	
3.1. Introduction.....	9
3.2. Hypabyssal kimberlite.....	9
3.3. Volcaniclastic kimberlite.....	10
4) Petrography of the Tuwawi Mantle Xenoliths	
4.1. Introduction.....	12
4.2. Coarse Peridotite.....	13
4.3. Deformed Peridotite	
4.3.1. Porphyroclastic Samples.....	13
4.3.2. Mosaic-Porphyroclastic Sample.....	14
4.4. Clinopyroxenite Sample.....	14

5) Mineral Chemistry of the Tuwawi Mantle Xenoliths	
5.1. Analytical Methods.....	16
5.2. Olivine.....	17
5.3. Orthopyroxene.....	17
5.4. Clinopyroxene.....	18
5.5. Garnet.....	18
5.6. Spinel.....	19
6) Geothermobarometry of Tuwawi Mantle Xenoliths.	
6.1. Geothermobarometers Used.....	26
6.2. Methodology of P-T Estimates.....	27
6.3. Results and Comparison with Literature Data.....	30
7) Diamond Potential of the Tuwawi Kimberlite.....	34
References.....	37
Appendix I	
A. Mantle Xenoliths.....	41
B. Kimberlites.....	49
Appendix II.....	58

## LIST OF FIGURES

---

Figure 1 – Map showing the locations of kimberlites discussed in this paper on Baffin and Somerset Islands, Nunavut.....	2
Figure 2 – Map of Palaeozoic geology of Brodeur Peninsula, also showing Brodeur Property claims and location of Tuvawik kimberlite.....	3
Figure 3 – Map of tectonic setting of Baffin Island.....	6
Figure 4a – Photo of hypabyssal texture.....	11
Figure 4b – Photo of contact between different matrices in volcanoclastic kimberlite sample.....	11
Figure 4c – Photo of light matrix in volcanoclastic kimberlite sample.....	11
Figure 4d – Photo of lapillus in dark matrix in volcanoclastic kimberlite sample.....	11
Figure 5a – Photo of coarse peridotite texture.....	15
Figure 5b – Photo of porphyroclastic peridotite texture.....	15
Figure 5c – Photo of mosaic-porphyroclastic peridotite texture.....	15
Figure 5d – Photo of clinopyroxenite sample.....	15
Figure 6 – Plot of P-T values calculated using all geothermobarometers.....	29
Figure 7 – Plot of P-T values calculated using the FB thermometer – MG barometer.....	31
Figure 8 – Plot of P-T values calculated using the BK thermometer – MG barometer.....	32
Figure 9 – Plot of P-T values calculated using the OW thermometer – MG barometer.....	32

## LIST OF TABLES

---

Table 1 – Minimum detection limits of electron microprobe analyses.....	16
Table 2 – Average composition of olivine from Tuwawi mantle xenoliths.....	20
Table 3 – Average composition of orthopyroxene from Tuwawi mantle xenoliths.....	21
Table 4 – Average composition of clinopyroxene from Tuwawi mantle xenoliths.....	22
Table 5 – Average composition of garnet from Tuwawi mantle xenoliths.....	23
Table 6 – Average composition of spinel from Tuwawi mantle xenoliths .....	24
Table 6 – Continued.....	25
Table 7 – Equilibrium pressure and temperature estimates for the Tuwawi mantle xenoliths.....	29

## **LIST OF APPENDICES**

---

Appendix I – Thin section descriptions.....	41
Appendix II – Electron microprobe analysis of mantle xenolith samples.....	58



## ACKNOWLEDGMENTS

---

First I'd like to thank Maya Kopylova, my supervisor, for her endless patience and help. Many thanks to David Ritcey and the rest of Diamondex Resources for letting me study their samples, without which this project would never have happened. Thanks to Mary Lou Bevier for providing so many resources, and Mati Raudsepp and Edith Czech for their help on the microprobe. Thank you to the Department of Earth and Ocean Sciences at UBC for helping with funding this project. Thank you also to my fellow honours students; this has been quite an experience that I'm glad to have shared with you. Lastly, I'd like to thank my parents for all the love and support.

# **CHAPTER 1**

## **INTRODUCTION**

---

### **1.1 INTRODUCTION**

It is important to recognize at an early stage in exploration whether a diamond deposit has the potential of being economic or not (Griffin and Ryan, 1995). The diamond potential of a kimberlite pipe is determined through detailed petrographic and chemical analyses, and the calculation of equilibrium pressures and temperatures to determine the depths of the mantle sampled by the kimberlite. These depths provide information about the probability of the kimberlite magma sampling diamonds; the thermal properties of the mantle below the surrounding area are also crucial. The textural classification of a kimberlite is another important process in determining its diamond potential. This paper presents the petrography, geochemistry, and geothermobarometry of the Tuwawi kimberlite and associated mantle xenoliths for the discussion and determination of the pipe's diamond potential.

### **1.2 LOCATION**

The Tuwawi kimberlite is one of three kimberlite occurrences found on the Brodeur Property of Baffin Island, Nunavut. This is the second kimberlite cluster found on the Brodeur Peninsula of Baffin Island, the first being the Freightrain (previously known as Zulu), discovered in 1975 by Cominco Ltd. (now owned by Atlanta Gold Corp.; Ritcey, unpublished, 2008). The Brodeur property is located approximately 100 km northwest of the Arctic Bay community (Fig. 1), and is claimed by Diamondex Resources Ltd. The property claims extend from 73.12° to 73.71° N latitude and 85.96 °to 88.36° W longitude (Fig.2), and are situated directly northeast of the Freightrain and Cargo kimberlites (Ritcey, unpublished, 2008).

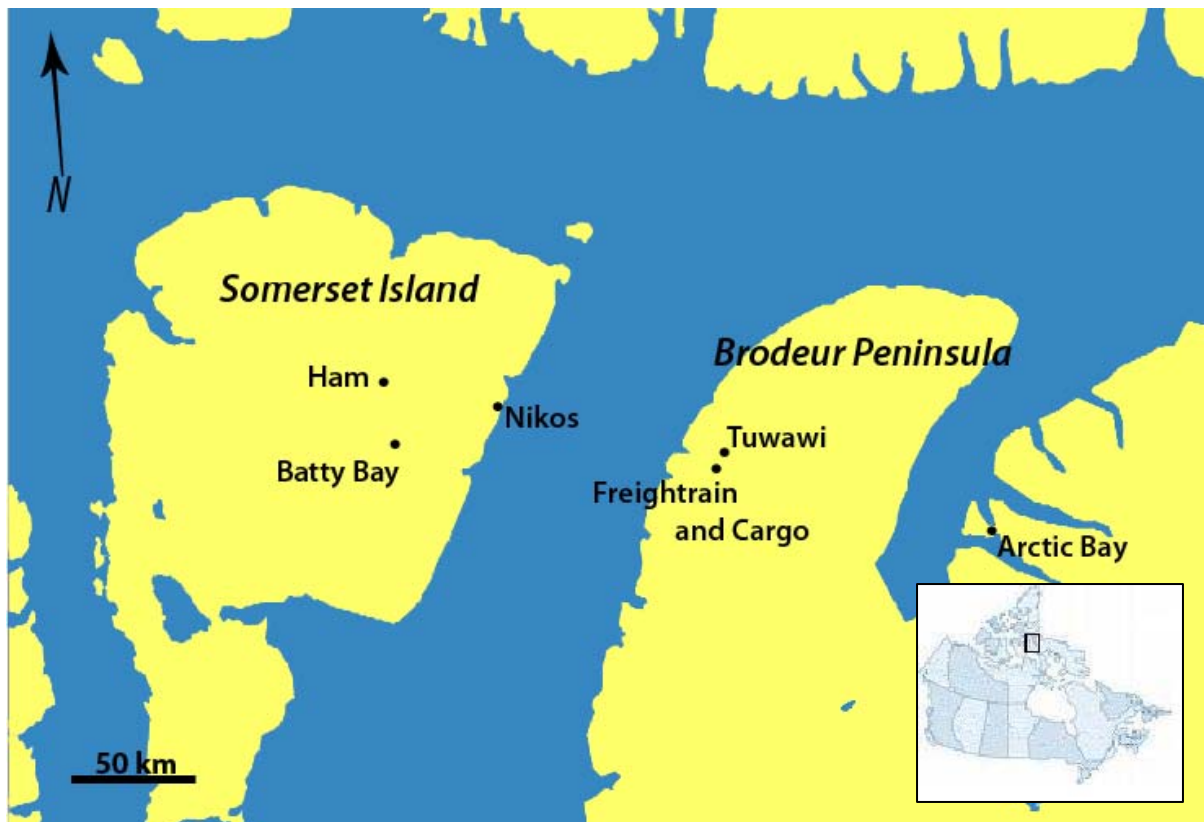


**Figure 1.** Map of Somerset Island and the Brodeur Peninsula of Baffin Island, Nunavut. Locations of kimberlite occurrences are shown. The community of Arctic Bay is also shown for reference.

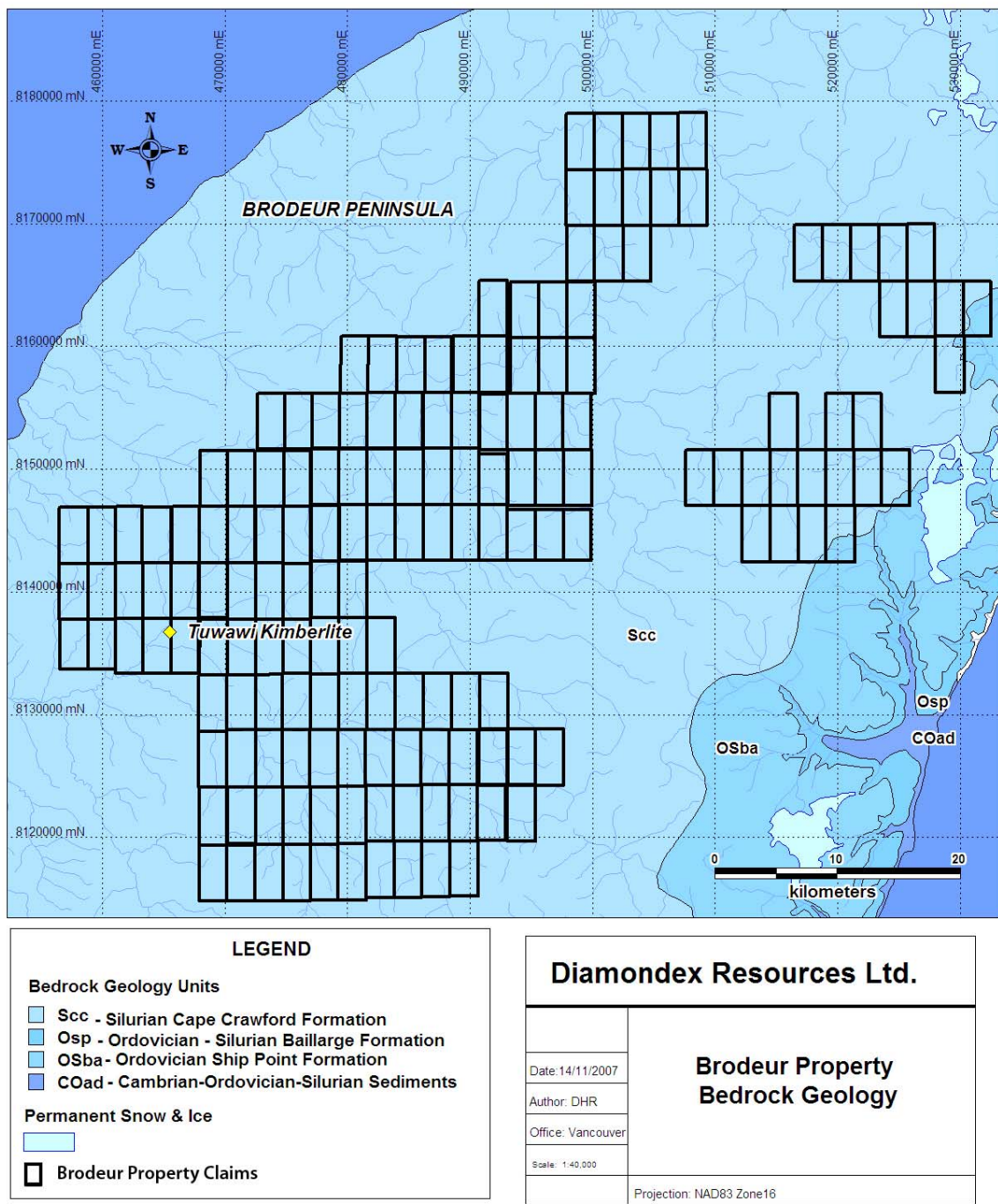


**Figure 2.** Palaeozoic geology of the area around the Brodeur Property. Modified from Ritcey, 2007.

### 1.3 PREVIOUS WORK

Jago et al. (2002) studied the Freightrain kimberlite; a pipe exposed in the crater facies with the presence of pyroclastics kimberlite indicating it is near the transition into diatreme facies. The kimberlite contains xenoliths of garnet and chromite harzburgite, garnet lherzolite, garnet spinel lherzolite and rare eclogite. An approximate geotherm of  $42 \text{ mW/m}^2$  was calculated using the geothermobarometry method of Nimis and Taylor (2000) for single clinopyroxene grains, and the majority of samples analyzed were found to originate in the diamond stability field. In comparison, kimberlites from Somerset Island are reported to have a hotter geotherm of approximately  $44 \text{ mW/m}^2$  and originate in the graphite stability field (Schmidberger and Francis, 1998; Jago and Mitchell, 1987; Kjarsgaard and Peterson, 1992). Among these kimberlites are the Ham, Nikos, and Batty Bay Complex, all located on the western edge of Somerset Island, and thought to of been emplaced during the Cretaceous (Heaman, 1989). Predating the study by Jago et al. (2002) was another done by Zhao et al. (1997) in which the Freightrain kimberlite (still called Zulu then) was dated and found to be of Cretaceous age. No previous work has been conducted on the Tuwuwi kimberlite, or the other kimberlites on the Brodeur Property (Nanuk and Kuuriaq).

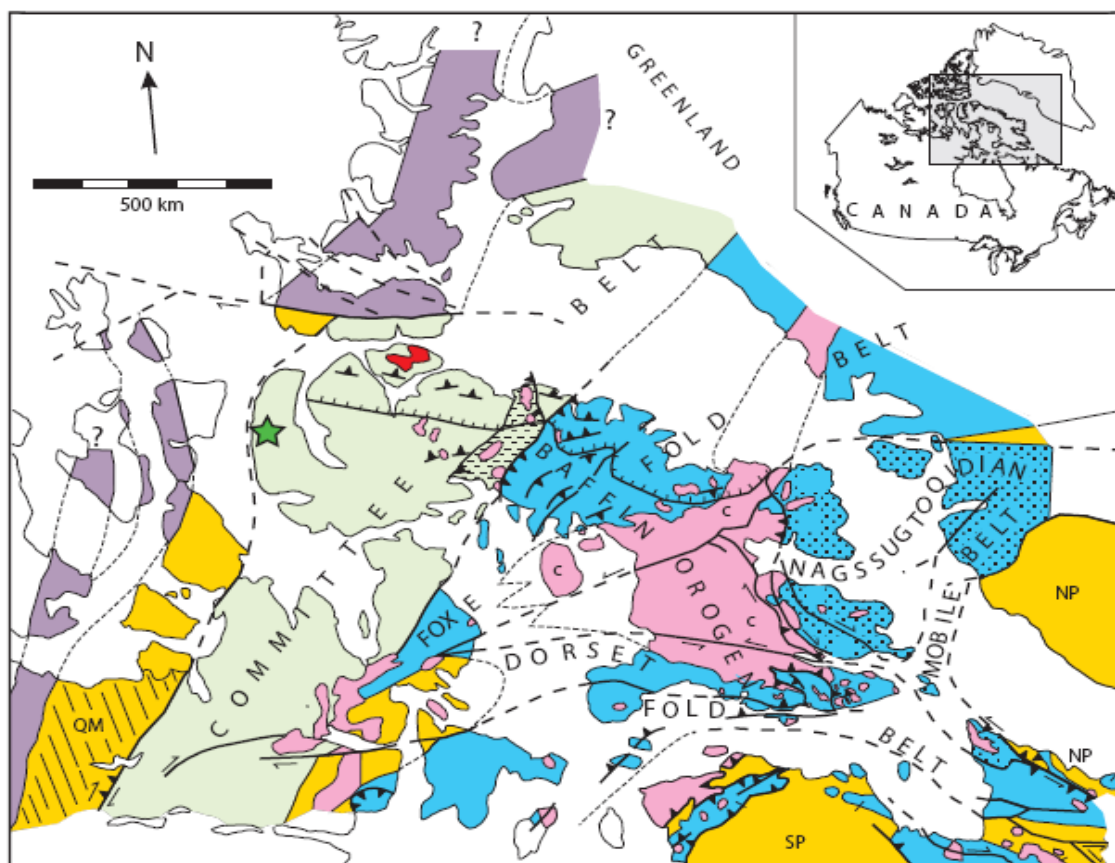
## **CHAPTER 2**

### **GEOLOGICAL SETTING**





---

#### **2.1 TECTONIC SETTING**




Baffin Island can be divided into two separate tectonic sections (Fig. 3). The Northern half of the island is composed of the Archean Committee Belt, a section of the Rae Domain (part of the Western Churchill Province). The rest of the Western Churchill Province is designated as the Hearne Domain and lies to the southwest of Baffin Island. To the northwest of the Rae Domain lies the Slave Craton, separated by the Thelon Tectonic Zone (Berman et al., 2005). The southern portion of Baffin Island is composed of the Paleoproterozoic Baffin Orogen which is a part of the Trans-Hudson Orogen. The Baffin Orogen is composed of a multitude of tectonic belts thrust upon one another. These include the Foxe Fold Belt, the Dorset Fold Belt and the Nagssugtoqidian Mobile Belt (Fig. 3).







#### PALEOPROTEROZOIC

-  Dexterity Granulite Belt (1.825 Ga); reworked Archean and some Paleoproterozoic rocks
-  Granite-tonalite, charnockite-enderbite plutons (1.87- 1.81 Ga, c= Cumberland Batholith)
-  Thelon Tectonic Zone; reworked Archean, 2.0 - 1.9 Ga granitic, and charnockitic intrusions, supracrustal rocks of uncertain age
-  Supracrustal rocks and derived gneisses (2.2 - 1.8 Ga); includes some small Paleoproterozoic granitic plutons, and reworked Archean rocks; Nagssugtoqidian Mobile Belt is shown by stippling

#### ARCHEAN

-  Granite - tonalite, charnockite - enderbite (~2.54 Ga)
  -  Committee Belt; 2.9-2.5 Ga granite-greenstone terranes with some older and younger rocks, and Paleoproterozoic reworking
  -  Undifferentiated Archean (3.8-2.5 Ga); local Paleoproterozoic reworking
- NP = Nain Province, SP = Superior Province, and QM = Queen Maud Block

#### MAJOR PALEOPROTEROZOIC STRUCTURES:

-  thrust
-  fault or shear zone (defined, assumed)
-  western limit of Northeast Baffin Thrust Belt (1.825-1.81 Ga)
-  location of Tuwawi Kimberlite

**Figure 3.** Tectonic setting of Baffin Island. Modified from Jackson and Berman (2000).

## 2.2 REGIONAL GEOLOGY

The Committee Belt (*ca.* 3.0–2.5 Ga) is characterized by episodic felsic plutonism and greenschist to upper amphibolite facies supracrustal belts. Three Archean crustal-building events characterize the Committee Belt. The oldest event (*ca.* 3.0 – 2.8 Ga), is represented by a *ca.* 2.85 Ga felsic pluton on northwestern Baffin Island and *ca.* 2.9 Ga felsic volcanic rocks to the southwest (Frisch, 1982). Widespread felsic plutonism and metavolcanic and paragneiss sequences (Jackson and Berman, 2000) characterize the second event, and the final event is represented by younger (*ca.* 2.6 – 2.5 Ga) granitic plutons and orthogneisses found in the southwestern section of the belt, as well as on islands to the north and northeast of Baffin Island. Subsequently a *ca.* 2.55–2.50 Ga tectonothermal event affected much of the Committee belt (Jackson and Berman, 2000), but did not contribute to it volumetrically.

Four major rock assemblages have been identified within the Committee Belt on northern Baffin Island (Jackson and Berman, 2000). Mesoarchean (< 2.9–2.8 Ga) rocks consist of felsic orthogneisses and foliated, strongly deformed felsic plutonic rocks. The Neoarchean assemblage (2.76–2.71 Ga) is represented by the supracrustal, syn- to late-tectonic felsic intrusions (Jackson and Berman 2000) of the Mary River group. Two Archean and/or Paleoproterozoic units consist of layered gneissic migmatite, and granite – charnockite; these are of uncertain age due to deformation, metamorphism, and plutonism in the Paleoproterozoic, making dating difficult (Jackson and Berman 2000). Thin sequences of Paleoproterozoic shelf quartzites and marble overlain by turbidites and wackes compose the Piling Group, which was deposited on exhumed Archean crust. Next, the Mesoproterozoic Bylot Supergroup was deposited in the Borden Rift Basin after uplift following Paleoproterozoic orogenesis (Jackson and Berman, 2000).

Thick sequences of Palaeozoic shallow marine platform and minor non-marine platform carbonate and clastic sedimentary rocks, as well as some deep water units (Trettin, 1969 and 1991) unconformably overly Archean and Proterozoic units in the area, and are in



turn unconformably overlain by unconsolidated Quaternary sedimentary deposits (Trettin, 1969, Ritcey, (unpublished) 2008).

## **2.3 LOCAL GEOLOGY**

Brodeur Peninsula is composed of Palaeozoic marine and non-marine platform sedimentary rocks (Fig. 2) underlain by Archean rocks of the Committee Belt. These Palaeozoic sedimentary rocks consist, in stratigraphic sequence, of the Admiralty Group of Cambrian and/or Early Ordovician age, the Early to Middle Ordovician Ship Point Formation, and the Brodeur Group of Ordovician and Silurian age (Trettin, 1969). The Admiralty Group is composed of two formations, the Gallery Formation, composed of quartzose and minor dolomitic sandstone, and the Turner Cliffs Formation, composed of a quartzose and dolomitic sandstone, and dolomitic, fine clastic sandstone. The Ship Point Formation is represented predominantly by pure dolomite (Trettin, 1969). The Brodeur Group is composed of the Baillarge and Cape Crauford Formations, a succession of Ordovician and Silurian self carbonates. The Cape Crauford Formation is unconformably overlain by unconsolidated Quaternary sediments (Trettin, 1969) consisting of a glacial till veneer and blanket, colluvial rubble from carbonates and consolidated clastics, and minor areas of glacio-marine and marine sediments. Units of the Baillarge and Cape Crauford formations underlie the mineral claims of the Brodeur property (Ritcey, (unpublished) 2008).

## **CHAPTER 3**

### **PETROGRAPHY OF THE TUWAWI KIMBERLITE**

---

#### **3.1 INTRODUCTION**

This section will describe the petrography of samples from the Tuwawi kimberlite. There are four samples (89486, 89488, 89495, and 89496). Two thin sections were made for each sample except sample 89488, for which only one thin section was made due to the low cohesiveness of the sample. The majority of the samples are hypabyssal textured, except 89488, which is of volcanoclastic texture. Hypabyssal kimberlite is characterised as non-fluidized intrusive rock formed from the slow crystallization of kimberlite magma (Scott Smith, 1996). Hypabyssal kimberlites are macroscopically uniform in most cases (Field and Scott Smith, 1999). The classification of volcanoclastic kimberlite is given to extrusively formed fragmental kimberlite deposits for which the process of deposition is unknown (Field and Scott Smith, 1999). Detailed thin section descriptions are in Appendix I.

#### **3.2 HYPABYSSAL KIMBERLITE**

The hypabyssal kimberlites consist of olivine macrocrysts ( $>0.5\text{mm}$ ; Scott Smith, 1996) and microphenocrysts ( $<0.5\text{mm}$ ) in a fine grained serpentine-calcite matrix (Fig.4a). All hypabyssal samples show olivine macrocrysts in similar abundance (13-14%). A few macrocrysts of spinel are also present, and sample 89495 has a small percentage of garnet grains with opaque kelyphitic rims; one as an inclusion in an olivine macrocryst. Olivine macrocrysts are present in subhedral rounded shapes and are fractured; some grains also show undulose extinction and dynamic recrystallization. This indicates a xenocrystal origin of olivine. Secondary serpentine, and minor calcite and chlorite, are present along fractures of the olivine macrocrysts. Surrounding the macrocrysts is a microcrystalline groundmass. Microphenocrysts of olivine are present in the groundmass, showing subhedral to euhedral grains with equant and elongate shapes. Also in the groundmass are serpentine, calcite,

spinel, perovskite, opaque minerals and some phlogopite. Calcite occurs as anhedral fine grained aggregates, as well as fibrous groundmass crystals. Serpentine also occurs as fine grained aggregates. Both minerals show a patchy distribution in sample 89486. Spinel is present in both bead and atoll form. Bead spinel refers to the small spinel grains that form around the grain boundaries of other minerals, mostly olivine microphenocrysts. Atoll spinel refers to spinel grains showing a cubic shape and having a cubic halo around the grain. Perovskite is also present, although not in as much abundance as spinel. Perovskite occurs as small, euhedral, equant grains (40  $\mu\text{m}$  to 0.16 mm). In sample 89495, there is a large anhedral perovskite grain (0.32x0.2 mm). The abundant tiny opaque grains most likely represent the finer grain fraction of spinel. Phlogopite is also present in the groundmass as euhedral laths ranging in size from 30x5  $\mu\text{m}$  to 0.6x0.08 mm.

### **3.3 VOLCANICLASTIC KIMBERLITE**

The volcaniclastic sample is composed of two irregularly intermixed matrices both containing discrete olivine macrocrysts and microphenocrysts, as well as lapilli. Only one area in the thin-section shows a clear contact between the two materials (Fig. 4.3b). The lighter matrix is composed of very fine grained, almost cryptocrystalline, carbonate and serpentine with minor spinel, phlogopite and opaque minerals (Fig. 4c). Lapilli are present in irregular shapes, and some are cored by olivine, or orthopyroxene, with thin selvages. The dark matrix material is also composed of cryptocrystalline carbonate and serpentine, except with a larger amount of spinel and opaque minerals (or ash) giving it a darker appearance (Fig. 4d). The majority of lapilli can be classified as juvenile rather than pelletal lapilli; as their olivine cores are surrounded by selvages of varying thickness and shape (Scott Smith, 1996). Few are olivine cored, and most form erratic shapes pertaining to the olivine grains within them. The selvages seem to be composed of the lighter matrix material. Olivine macrocrysts and microphenocrysts within the sample show a restricted size distribution in comparison to those in hypabyssal kimberlite. The smaller grains have a very uniform size of  $\sim 160 \mu\text{m}$ . This is one line of evidence supporting a volcaniclastic texture for this sample. Other evidence includes the angular shapes of the olivines, the presence of lapilli and the unusually dark and cryptocrystalline nature of the matrices.

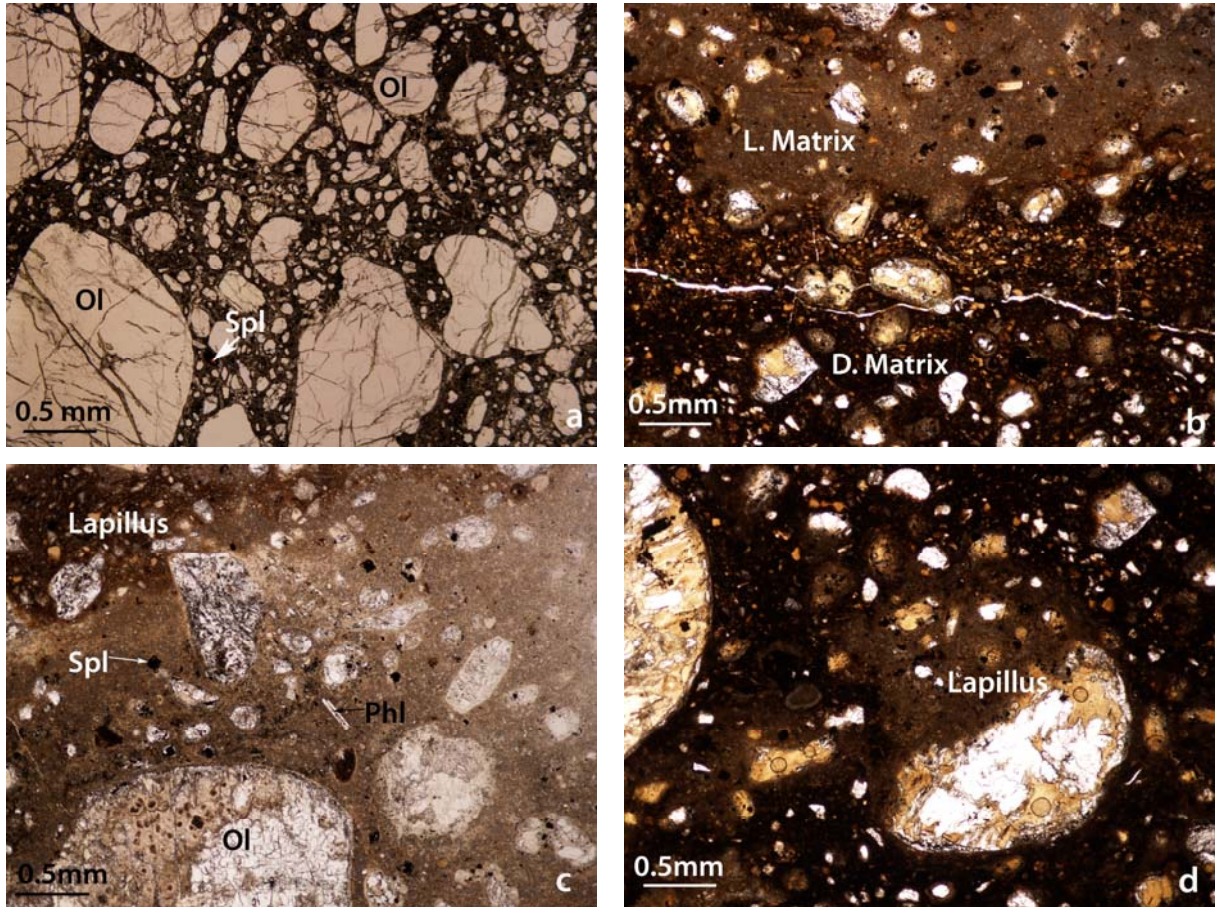


**Figure 4.** Microscope photos of kimberlite textures. a) Hypabyssal kimberlite; b) Contact between light and dark matrix of volcanoclastic kimberlite; c) Light matrix of volcanoclastic kimberlite; d) Juvenile lapillus in the dark matrix of volcanoclastic kimberlite. L.Matrix=light matrix, D.Matrix=dark matrix, Ol=olivine, Spl=spinel, Phl=phlogopite.

## CHAPTER 4

### PETROGRAPHY OF THE TUWAWI MANTLE XENOLITHS

---

#### 4.1 INTRODUCTION

This section will describe the petrography of the mantle xenoliths found in samples from the Tuwawi kimberlite. There are five samples (89481, 89487, 89490, 89494, and 89497) with six xenoliths. A thin section was made for each sample except sample 89490 for which two thin sections were made, due to the presence of two different xenoliths (89490B xenolith A and B). The samples are all of peridotitic composition, except 89481, which is clinopyroxenite. Detailed thin section descriptions are in Appendix I.

After petrographic analysis of the six thin sections, a range of textures and mineralogy has been identified. The samples, excluding the clinopyroxenite, have been divided into three textural groups (Figures 5a-c) after Harte (1977): porphyroclastic (89490B xenolith B, 89494), mosaic-porphyroclastic (89490A and 89490B xenolith A), and coarse (89487, 89497). An increase in the evidence of recrystallization corresponds to an increase in deformation to the sample. Mosaic-porphyroclastic samples are more deformed than porphyroclastic, and coarse samples have experienced very minimal deformation, or none at all (Nixon et al., 1981). Porphyroclastic textures are characterized by the presence of porphyroclasts (large strained grains completely surrounded by smaller grains) of which there is a proportion greater than 10% to that of the finer grained matrix (Harte, 1977). The smaller grains making up the matrix and surrounding the porphyroclasts are called “neoblasts” (Nicholas et al., 1971). These grains are generally polygonal or tabular showing little strain and are believed to occur from recrystallization. Mosaic-porphyroclastic texture is characterized by the presence of porphyroclasts and a proportion of greater than 90% neoblasts to porphyroclasts (Harte, 1977). Neoblast grains occur in equant hexagonal shapes producing a mosaic look to the matrix. Coarse textures lack porphyroclasts, and the majority of mineral grains are on the order of 2 mm or greater in diameter showing straight, smoothly

curved or less regular grain boundaries (Harte, 1977). The clinopyroxenite xenolith is too altered for a representative texture to be identified (Fig. 5d). The mosaic-porphyroclastic xenoliths found in thin sections 89490A and 89490B (xenolith A) are determined to be from the same xenolith sample and thus from now on will only be referred to as sample 89490. The other xenolith in thin section 89490B (xenolith B) will be referred to as 89490B.

## **4.2 COARSE PERIDOTITE**

The coarse peridotites are composed of olivine (82-84%), orthopyroxene (10-12%), clinopyroxene (1-3%) and spinel (1-3%) with varied amounts of garnet (0-5%) (Fig. 5a). Rock types include garnet-spinel harzburgite and spinel harzburgite, according to the IUGS classification triangle for ultramafic rocks consisting essentially of olivine, orthopyroxene and clinopyroxene. Grains of olivine and pyroxene are anhedral, mostly equant with some elongate shapes. Olivine and orthopyroxene grains are highly fractured showing undulose extinction, and some of the larger orthopyroxenes have deformational twinning present. Spinel is anhedral and forms interstitially in sample 89497. The clinopyroxene present in sample 89487 almost exclusively occurs in association with spinel grains, whereas in sample 89497 it occurs in association with orthopyroxene, sometimes even in solid solution equilibrium. Garnet, only present in sample 89497, is mostly all completely recrystallized to kelyphite; a microcrystalline aggregate of spinel, phlogopite, chlorite, amphibole, and (?)plagioclase that develops at the garnet's expense (Dawson and Stephens, 1975).

## **4.3 DEFORMED PERIDOTITE**

### **4.3.1 Porphyroclastic Samples**

The porphyroclastic xenoliths are composed of olivine (85-97%), orthopyroxene (3-8%), clinopyroxene (0-5%), and garnet (0-2%) (Fig. 5b). Rock types include garnet lherzolite and dunite. The porphyroclastic texture is due to dynamic recrystallization of olivine grains forming subhedral to anhedral olivine porphyroclasts and anhedral neoblasts. Olivine porphyroclasts show deformation

structures such as undulose extinction, and fluidal inclusions following fracture patterns. Anhedral orthopyroxene and euhedral to subhedral clinopyroxene grains show evidence of deformation such as undulose extinction. Inclusions are also present around grain boundaries, indicative of partial melting. Garnet is only present in sample 89494, and has been almost completely recrystallized to kelyphite. The dunite xenolith is only represented by a very small section present in sample 89490B, and so this petrographic/mineralogical classification must be considered only tentative as a larger sample could prove to show a different composition than seen here.

#### **4.3.2 Mosaic-Porphyroclastic Sample**

The mosaic-porphyroclastic xenolith is composed of olivine (70%), orthopyroxene (15-20%), clinopyroxene (10%), and garnet (5%) (Fig. 5c). The rock type is garnet lherzolite. Anhedral olivine porphyroclasts commonly show undulose extinction, and neoblasts are present in anhedral equant hexagonal shapes giving the rock the characteristic “mosaic” texture. Orthopyroxene and clinopyroxene also show porphyroclasts and neoblasts, as well as evidence for partial melting, such as inclusions along grain margins. All garnet grains are surrounded by a kelyphitic rim, although these are the thinnest of all the peridotite samples analyzed.

#### **4.4 CLINOPYROXENITE SAMPLE**

The clinopyroxenite xenolith consists of garnet (20%), clinopyroxene (10%) and minor orthopyroxene (1%), spinel (0.5%) and olivine (0.5%) (Fig.5d). The sample is highly altered (70%) by a cryptocrystalline material likely to be serpentine and chlorite, making it difficult to determine a texture to the rock. Garnet grains have recrystallized kelyphitic rims. Clinopyroxenes show high birefringence and fracturing.



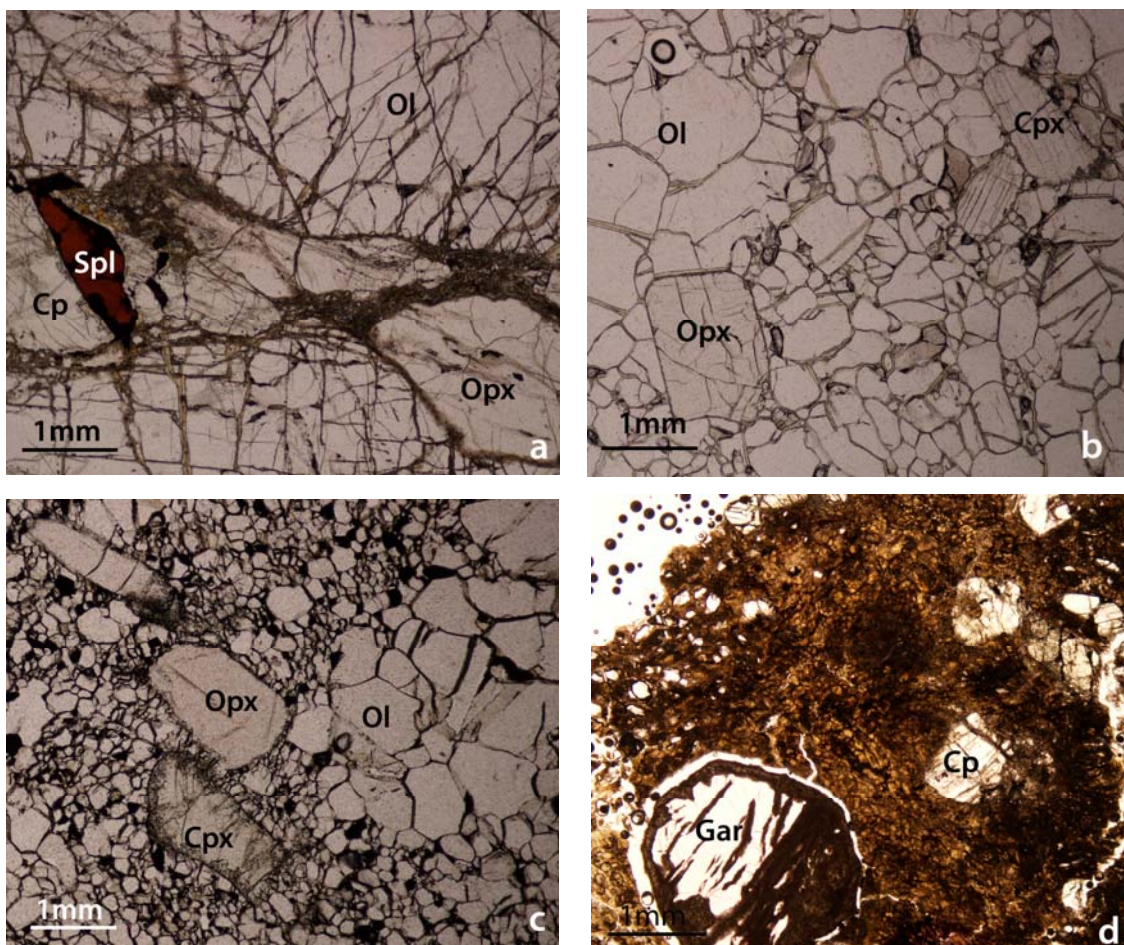


**Figure 5.** Microscope photos of textures and rocks described above. a) Coarse texture (sample 89487); b) Porphyroclastic texture (sample 89494); c) Mosaic-porphyroclastic texture (sample 89490); d) Clinopyroxenite (sample 89481). Ol=olivine, Opx=orthopyroxene, Cpx=clinopyroxene, Gar=garnet, Spl=spinel.



## CHAPTER 5

### MINERAL CHEMISTRY OF THE TUWAWI MANTLE XENOLITHS

---

#### 5.1 ANALYTICAL METHODS

Electron Microprobe analysis was conducted all six mantle xenolith samples at the University of British Columbia, Earth and Ocean Science Department using a fully-automated Cameca SX-50 Scanning Electron Microprobe, operating on wavelength dispersion mode (WDS). Olivine, pyroxene, garnet and spinel were analyzed at an excitation voltage of 15 kV and a beam current of 20 nA. For all elements peak count times were 20 s, with the exception of K in pyroxene and Na in garnet which were 40 s and 60 s respectively. Background count times were 10 s for all elements, except K in pyroxene and Na in garnet which were 20 s and 30 s. For all elements analyzed the spot diameter was 5  $\mu\text{m}$ . Data reduction was done using the 'PAP'  $\phi(\rho Z)$  method (Pouchou & Pichoir, 1985). The above analytical conditions and counting times resulted in the following minimum detection limits:

**Table 1 Minimum Detection Limits  
for Electron Microprobe Analyses**

Oxides	MDL (wt %)
SiO <sub>2</sub>	0.07
TiO <sub>2</sub>	0.05
Al <sub>2</sub> O <sub>3</sub>	0.09
Cr <sub>2</sub> O <sub>3</sub>	0.16
FeO	0.08
MnO	0.08
MgO	0.04
CaO	0.04
Na <sub>2</sub> O	0.09
K <sub>2</sub> O	0.09
NiO	0.09

## 5.2 OLIVINE

Olivines in all xenoliths are forsterite-rich, with Mg# of 0.91 and 0.92 ( $\text{Mg\#} = \text{Mg}/(\text{Mg}+\text{Fe})$ ; Table 2). There is no obvious chemical distinction between neoblasts and porphyroclasts in deformed xenoliths. Deformed peridotites have olivines with slightly lower MgO and higher FeO (49.72-49.57 wt% MgO, 8.97-8.93 wt% FeO) than those in coarse samples (50.81-50.71 wt% MgO, 7.37-7.53 wt% FeO). The porphyroclastic xenolith in sample 89490B has olivines with MgO and FeO values between those in the other deformed xenoliths and the coarse xenoliths (50.53 wt% MgO, 8.04 wt% FeO). Xenoliths containing spinel also show the trend of having olivine grains with higher MgO and lower FeO than those in xenoliths without spinel. Nickel content is basically homogeneous in all olivines (0.37-0.39 wt% NiO), except sample 89497 in which grains have a NiO content of 0.34 wt% NiO. All olivines are Al, Cr, Ti and Na-poor with  $\text{Al}_2\text{O}_3$ ,  $\text{Cr}_2\text{O}_3$ ,  $\text{TiO}_2$  and  $\text{Na}_2\text{O}$  all below minimum detection limits (MDL).

## 5.3 ORTHOPYROXENE

Orthopyroxenes are all enstatite rich with Mg# of 0.92-0.93 (Table 3), and have similar FeO content (5.06-5.62 wt% FeO). The exception is sample 89497, in which orthopyroxenes have a lower FeO value of 4.63 wt% FeO. Coarse peridotites and clinopyroxenite show grains slightly more Mg-rich (34.74-36.23 wt% MgO) than those in deformed peridotites (33.99-34.67 wt% MgO). Chemical compositions, with regards to  $\text{Al}_2\text{O}_3$  content, show orthopyroxenes in deformed xenoliths with higher  $\text{Al}_2\text{O}_3$  (0.76-0.68 wt%  $\text{Al}_2\text{O}_3$ ) than those in the clinopyroxenite (0.56 wt%  $\text{Al}_2\text{O}_3$ ) and one of the coarse xenoliths (89497) (0.63 wt%  $\text{Al}_2\text{O}_3$ ). The other coarse sample (89487) has very Al-rich (1.71 wt%  $\text{Al}_2\text{O}_3$ ) orthopyroxenes. Chromium content is homogeneous across all orthopyroxene (0.21-0.23 wt%  $\text{Cr}_2\text{O}_3$ ) except sample 89487, in which the  $\text{Cr}_2\text{O}_3$  content of orthopyroxene is approximately double (0.41 wt%  $\text{Cr}_2\text{O}_3$ ). Orthopyroxenes in coarse samples show  $\text{TiO}_2$  levels below MDL; all other orthopyroxenes are Ti-poor (0.11-0.22 wt%  $\text{TiO}_2$ ).

## 5.4 CLINOPYROXENE

Clinopyroxenes are Ti-poor ( $< \text{MDL}-0.16 \text{ wt\% TiO}_2$ ) Cr-diopside ( $0.80-1.36 \text{ wt\% Cr}_2\text{O}_3$ ; Table 4) except sample 89494, in which grains show a  $\text{TiO}_2$  content of  $0.31 \text{ wt\%}$ . Clinopyroxenite has clinopyroxenes with slightly higher  $\text{Cr}_2\text{O}_3$  content ( $1.36 \text{ wt\% Cr}_2\text{O}_3$ ), than those in peridotite samples ( $0.80-0.98 \text{ wt\% Cr}_2\text{O}_3$ ). Grains in deformed peridotite xenoliths and clinopyroxenite are slightly Ca-poor ( $\text{Ca\#} = \text{Ca}/(\text{Ca}+\text{Mg}) = 0.42-0.44$ ), whereas in coarse xenoliths calcium is slightly higher ( $\text{Ca\#} = 0.49$ ). Deformed peridotites and clinopyroxenite show clinopyroxenes with similar values of FeO ( $2.69-3.16 \text{ wt\% FeO}$ ), and coarse peridotites show Fe-poor grains ( $1.19-1.54 \text{ wt\% FeO}$ ). Clinopyroxenes in clinopyroxenite are slightly richer in  $\text{Na}_2\text{O}$  ( $1.60 \text{ wt\% Na}_2\text{O}$ ) than those found in peridotites ( $0.58-1.10 \text{ wt\% Na}_2\text{O}$ ). Sodium content is lower in coarse peridotite samples compared to deformed ones. Coarse peridotite grains have similar MgO content to those in clinopyroxenite ( $17.30-17.60 \text{ wt\% MgO}$ ), whereas in deformed peridotite xenoliths clinopyroxenes are Mg-rich ( $18.90-18.94 \text{ wt\% MgO}$ ).

## 5.5 GARNET

Garnets in all xenoliths are Ti-poor pyrope (Group 9 of Dawson and Stephens 1975, Table 5), except for one Ti-rich pyrope (Group 1 of Dawson and Stephens 1975; sample 89490). Group 1 garnets are determined to be from sheared-lherzolites. Group 9 garnets are determined to be from granular lherzolites, and can also include those from sheared-lherzolites. This is consistent with the petrography of the samples; sample 89490 is the only mosaic-porphyroclastic xenolith. Garnets in coarse peridotite are Al and Mg-poor ( $18.89 \text{ wt\% Al}_2\text{O}_3$ ,  $17.69 \text{ wt\% MgO}$ ) and Cr and Ca-rich ( $7.24 \text{ wt\% Cr}_2\text{O}_3$ ,  $7.13 \text{ wt\% CaO}$ ) with respect to deformed peridotites and clinopyroxenite ( $20.98-21.64 \text{ wt\% Al}_2\text{O}_3$ ,  $20.74-21.11 \text{ wt\% MgO}$ ,  $2.70-3.40 \text{ wt\% Cr}_2\text{O}_3$ ,  $4.48-4.56 \text{ wt\% CaO}$ ). Iron contents are similar throughout all xenoliths ( $7.22-7.69 \text{ wt\% FeO}$ ), with garnets in deformed peridotites showing the highest and lowest values corresponding respectively to mosaic and porphyroclastic textures. Coarse peridotites have garnets showing  $\text{TiO}_2$  contents below MDL, whereas other xenoliths show garnet grains with  $\text{TiO}_2$  values of  $0.35$  to  $0.46 \text{ wt\% TiO}_2$ .

## 5.6 SPINEL

Spinel has chemical compositions with significant intra-grain heterogeneity (Table 6). Within sample 89487, spinels are Ti-poor ( $< \text{MDL}$ ) aluminous ferrous magnesiochromites (av.  $\text{Mg}/(\text{Mg}+\text{Fe})$  of 0.63, av.  $\text{Cr}/(\text{Cr}+\text{Al})$  of 0.57). Iron content ranges from 13.22 to 15.53 wt % FeO. One rim analysis is Ni-rich (0.13 wt% NiO), while all other analyses show NiO contents below or at MDL. Spinel in sample 89497 is also aluminous ferrous magnesiochromite, but is slightly more Cr-rich (av.  $\text{Cr}/(\text{Cr}+\text{Al})$  of 0.74) and Ti-rich ( $< \text{MDL} - 1.05$  wt%  $\text{TiO}_2$ ). Nickel contents vary from below MDL to 0.17 wt% NiO. Aluminum content varies from 11.68 to 14.56 wt%  $\text{Al}_2\text{O}_3$ . One rim analysis is Ti-rich and Al-poor (1.05 wt%  $\text{TiO}_2$ , 11.68 wt%  $\text{Al}_2\text{O}_3$ ), while another rim analysis is Fe-rich ( $\text{Fe}/(\text{Fe}+\text{Mg}) = 0.40$ ).

**Table 2. Average Composition of Olivine from Tuwawi Mantle Xenoliths**

<b>Sample</b>	<b>89490</b>	<b>89494</b>	<b>89487</b>	<b>89497</b>	<b>89490B-b</b>
	core=rim	core=rim	core=rim	core=rim	core=rim
<b>no. avg.</b>	13	19	8	7	11
<b>SiO<sub>2</sub></b>	40.56	40.76	41.22	41.18	40.72
<b>TiO<sub>2</sub></b>	--	--	--	--	--
<b>Al<sub>2</sub>O<sub>3</sub></b>	--	--	--	--	--
<b>Cr<sub>2</sub>O<sub>3</sub></b>	--	--	--	--	--
<b>FeO</b>	8.97	8.93	7.37	7.53	8.04
<b>MnO</b>	0.11	0.10	0.08	0.10	0.12
<b>MgO</b>	49.72	49.57	50.81	50.71	50.53
<b>CaO</b>	0.07	0.06	--	0.04	0.07
<b>Na<sub>2</sub>O</b>	--	--	--	--	--
<b>K<sub>2</sub>O</b>	n/a	n/a	n/a	n/a	n/a
<b>NiO</b>	0.37	0.39	0.37	0.34	0.38
<b>Total</b>	99.89	99.91	99.91	99.95	99.98
<b>Oxygens</b>	4	4	4	4	4
<b>Si<sup>4+</sup></b>	1.000	1.000	1.000	1.000	1.000
<b>Ti<sup>4+</sup></b>	--	--	--	--	--
<b>Al<sup>3+</sup></b>	--	--	--	--	--
<b>Cr<sup>3+</sup></b>	--	--	--	--	--
<b>Fe<sup>2+</sup></b>	0.185	0.183	0.149	0.153	0.165
<b>Mn<sup>2+</sup></b>	0.002	0.002	0.002	0.002	0.003
<b>Mg<sup>2+</sup></b>	1.827	1.813	1.837	1.836	1.849
<b>Ca<sup>2+</sup></b>	0.002	0.002	--	0.001	0.002
<b>Na<sup>+</sup></b>	--	--	--	--	--
<b>K<sup>+</sup></b>	n/a	n/a	n/a	n/a	n/a
<b>Ni<sup>2+</sup></b>	0.007	0.008	0.007	0.007	0.008
<b>Total</b>	3.026	3.010	2.997	2.999	3.030
<b>Mg#</b>	0.91	0.91	0.92	0.92	0.92

Here and Further:

-- = below MDL

n/a = not analysed

**Table 3. Average Composition of Orthopyroxene from Tuwawi Mantle Xenoliths**

<b>Sample</b>	<b>89490</b>	<b>89494</b>	<b>89481</b>	<b>89487</b>	<b>89497</b>
	core=rim	core=rim	core=rim	core=rim	core=rim
<b>no. avg.</b>	1	18	4	1	18
<b>SiO<sub>2</sub></b>	57.30	56.95	57.30	56.93	57.28
<b>TiO<sub>2</sub></b>	0.12	0.22	0.13	--	--
<b>Al<sub>2</sub>O<sub>3</sub></b>	0.75	0.68	0.56	1.71	0.63
<b>Cr<sub>2</sub>O<sub>3</sub></b>	0.24	0.23	0.21	0.41	0.22
<b>FeO</b>	5.59	5.37	5.17	5.06	4.63
<b>MnO</b>	0.14	0.12	0.12	0.12	0.12
<b>MgO</b>	33.95	34.67	35.19	34.74	36.23
<b>CaO</b>	0.88	0.94	0.61	0.45	0.24
<b>Na<sub>2</sub>O</b>	0.17	0.13	0.11	--	--
<b>K<sub>2</sub>O</b>	--	--	--	--	--
<b>NiO</b>	n/a	n/a	n/a	n/a	n/a
<b>Total</b>	99.15	99.32	99.41	99.47	99.37
<b>Oxygens</b>	6	6	6	6	6
<b>Si<sup>4+</sup></b>	1.988	1.974	1.980	1.963	1.973
<b>Ti<sup>4+</sup></b>	0.003	0.006	0.003	--	--
<b>Al<sup>3+</sup></b>	0.031	0.028	0.023	0.069	0.026
<b>Cr<sup>3+</sup></b>	0.007	0.006	0.006	0.011	0.006
<b>Fe<sup>2+</sup></b>	0.162	0.156	0.149	0.146	0.134
<b>Mn<sup>2+</sup></b>	0.004	0.004	0.004	0.004	0.003
<b>Mg<sup>2+</sup></b>	1.756	1.791	1.812	1.785	1.860
<b>Ca<sup>2+</sup></b>	0.033	0.035	0.023	0.017	0.009
<b>Na<sup>+</sup></b>	0.011	0.009	0.007	--	--
<b>K<sup>+</sup></b>	--	--	--	--	--
<b>Ni<sup>2+</sup></b>	n/a	n/a	n/a	n/a	n/a
<b>Total</b>	3.996	4.008	4.007	3.998	4.012
<b>Mg#</b>	0.92	0.92	0.92	0.92	0.93

**Table 4. Average Composition of Clinopyroxene from Tuwawi Mantle Xenoliths**

<b>Sample</b>	<b>89490</b>	<b>89494</b>	<b>89481</b>	<b>89487</b>	<b>89497</b>
	core=rim	core=rim	core=rim	core=rim	core=rim
<b>no. avg.</b>	<b>1</b>	<b>3</b>	<b>1</b>	<b>1</b>	<b>3</b>
<b>SiO<sub>2</sub></b>	54.32	54.33	54.87	53.82	54.11
<b>TiO<sub>2</sub></b>	0.16	0.31	0.14	--	--
<b>Al<sub>2</sub>O<sub>3</sub></b>	0.65	1.50	2.00	1.89	0.99
<b>Cr<sub>2</sub>O<sub>3</sub></b>	0.96	0.80	1.36	0.98	0.85
<b>FeO</b>	2.94	3.16	2.69	1.54	1.19
<b>MnO</b>	0.11	0.12	0.11	0.08	0.06
<b>MgO</b>	18.90	18.94	17.38	17.30	17.60
<b>CaO</b>	19.99	18.71	19.01	22.86	23.68
<b>Na<sub>2</sub>O</b>	0.79	1.10	1.60	0.58	0.65
<b>K<sub>2</sub>O</b>	--	--	--	--	--
<b>NiO</b>	n/a	n/a	n/a	n/a	n/a
<b>Total</b>	98.82	99.04	99.21	99.05	99.13
<b>Oxygens</b>	<b>6</b>	<b>6</b>	<b>6</b>	<b>6</b>	<b>6</b>
<b>Si<sup>4+</sup></b>	1.986	1.977	1.992	1.965	1.976
<b>Ti<sup>4+</sup></b>	0.004	0.009	0.004	--	--
<b>Al<sup>3+</sup></b>	0.028	0.064	0.086	0.081	0.042
<b>Cr<sup>3+</sup></b>	0.028	0.023	0.039	0.028	0.024
<b>Fe<sup>2+</sup></b>	0.090	0.096	0.082	0.047	0.036
<b>Mn<sup>2+</sup></b>	0.003	0.004	0.003	0.002	0.002
<b>Mg<sup>2+</sup></b>	1.030	1.028	0.940	0.941	0.958
<b>Ca<sup>2+</sup></b>	0.783	0.730	0.739	0.894	0.927
<b>Na<sup>+</sup></b>	0.056	0.078	0.112	0.041	0.046
<b>K<sup>+</sup></b>	--	--	--	--	--
<b>Ni<sup>2+</sup></b>	n/a	n/a	n/a	n/a	n/a
<b>Total</b>	4.010	4.011	3.999	4.001	4.013
<b>Mg#</b>	0.92	0.91	0.92	0.95	0.96
<b>Ca#</b>	0.43	0.42	0.44	0.49	0.49

**Table 5. Average Composition of Garnet from Tuwawi Mantle Xenoliths**

<b>Sample</b>	<b>89490</b>	<b>89494</b>	<b>89481</b>	<b>89497</b>
	core=rjm	core=rjm	core=rjm	core=rjm
<b>no. avg.</b>	11	5	10	5
<b>SiO<sub>2</sub></b>	41.73	41.85	41.79	40.84
<b>TiO<sub>2</sub></b>	0.46	0.35	0.37	--
<b>Al<sub>2</sub>O<sub>3</sub></b>	20.98	21.64	21.27	18.89
<b>Cr<sub>2</sub>O<sub>3</sub></b>	3.07	2.70	3.40	7.24
<b>FeO</b>	7.69	7.22	7.36	7.53
<b>MnO</b>	0.30	0.29	0.32	0.49
<b>MgO</b>	20.77	21.11	20.74	17.69
<b>CaO</b>	4.55	4.48	4.56	7.13
<b>Na<sub>2</sub>O</b>	--	--	--	--
<b>K<sub>2</sub>O</b>	n/a	n/a	n/a	n/a
<b>NiO</b>	n/a	n/a	n/a	n/a
<b>Total</b>	99.60	99.68	99.86	99.81
<b>Oxygens</b>	7	7	7	7
<b>Si<sup>4+</sup></b>	2.990	2.985	2.984	2.981
<b>Ti<sup>4+</sup></b>	0.025	0.019	0.020	--
<b>Al<sup>3+</sup></b>	1.772	1.818	1.790	1.625
<b>Cr<sup>3+</sup></b>	0.174	0.152	0.192	0.418
<b>Fe<sup>2+</sup></b>	0.461	0.431	0.439	0.459
<b>Mn<sup>2+</sup></b>	0.018	0.017	0.020	0.030
<b>Mg<sup>2+</sup></b>	2.219	2.244	2.208	1.925
<b>Ca<sup>2+</sup></b>	0.349	0.342	0.349	0.558
<b>Na<sup>+</sup></b>	--	--	--	--
<b>K<sup>+</sup></b>	n/a	n/a	n/a	n/a
<b>Ni<sup>2+</sup></b>	n/a	n/a	n/a	n/a
<b>Total</b>	8.016	8.014	8.008	7.997
<b>Mg#</b>	0.83	0.84	0.83	0.81



**Table 6. Average Composition of Spinel from Tuwawi Mantle Xenoliths**

Sample	89497							
	core	rim	rim	core	core	rim	core	rim
no. avg.	3	1	1	3	1	1	2	1
<b>SiO<sub>2</sub></b>	--	--	--	--	--	0.08	--	--
<b>TiO<sub>2</sub></b>	--	0.10	0.05	--	0.07	1.05	--	0.64
<b>Al<sub>2</sub>O<sub>3</sub></b>	14.35	13.51	14.53	14.56	14.14	11.68	13.70	12.55
<b>Cr<sub>2</sub>O<sub>3</sub></b>	57.76	56.83	57.19	56.86	57.44	56.64	56.92	56.72
<b>FeO</b>	12.97	14.36	13.24	13.14	13.26	15.52	14.69	15.82
<b>MnO</b>	0.09	--	0.09	0.10	0.09	0.12	0.16	0.18
<b>MgO</b>	14.54	14.48	14.33	14.33	14.41	14.07	13.48	13.59
<b>CaO</b>	--	0.04	--	0.04	--	0.04	--	--
<b>Na<sub>2</sub>O</b>	n/a	n/a	n/a	n/a	n/a	n/a	n/a	n/a
<b>K<sub>2</sub>O</b>	n/a	n/a	n/a	n/a	n/a	n/a	n/a	n/a
<b>NiO</b>	--	0.11	--	--	0.11	0.17	--	0.10
<b>Total</b>	99.88	99.51	99.55	99.17	99.59	99.36	99.10	99.67
<b>Grain</b>	1&3	3	1	2&9	8	8	7	7
<b>Oxygens</b>	4	4	4	4	4	4	4	4
<b>Si<sup>4+</sup></b>	--	--	--	--	--	0.003	--	--
<b>Ti<sup>4+</sup></b>	--	0.002	0.001	--	0.002	0.026	--	0.016
<b>Al<sup>3+</sup></b>	0.534	0.508	0.543	0.545	0.529	0.445	0.519	0.476
<b>Cr<sup>3+</sup></b>	1.442	1.435	1.433	1.429	1.441	1.447	1.447	1.444
<b>Fe<sup>2+</sup></b>	0.343	0.384	0.351	0.349	0.352	0.419	0.395	0.426
<b>Mn<sup>2+</sup></b>	0.002	--	0.003	0.003	0.003	0.003	0.004	0.005
<b>Mg<sup>2+</sup></b>	0.684	0.689	0.677	0.679	0.682	0.678	0.646	0.652
<b>Ca<sup>2+</sup></b>	--	0.002	--	0.001	--	0.001	--	--
<b>Na<sup>+</sup></b>	n/a	n/a	n/a	n/a	n/a	n/a	n/a	n/a
<b>K<sup>+</sup></b>	n/a	n/a	n/a	n/a	n/a	n/a	n/a	n/a
<b>Ni<sup>2+</sup></b>	--	0.003	--	--	0.003	0.004	--	0.003
<b>Total</b>	3.010	3.025	3.010	3.011	3.012	3.026	3.016	3.023
<b>Mg#</b>	0.67	0.64	0.66	0.66	0.66	0.62	0.62	0.60
<b>Cr#</b>	0.73	0.74	0.73	0.72	0.73	0.76	0.74	0.75
<b>Fe#</b>	0.33	0.36	0.34	0.34	0.34	0.38	0.38	0.40

Table 6. Continued

Sample	89487									
	core	core	rim	rim	core	rim	rim	core	rim	rim
no. avg.	1	1	1	1	1	1	1	1	1	1
SiO <sub>2</sub>	--	--	0.48	--	--	--	0.43	--	--	--
TiO <sub>2</sub>	--	--	--	--	--	--	--	--	--	--
Al <sub>2</sub> O <sub>3</sub>	25.04	25.43	24.93	24.45	24.82	23.22	22.97	26.74	20.53	24.20
Cr <sub>2</sub> O <sub>3</sub>	45.36	44.93	44.76	45.64	46.01	46.43	45.82	43.51	50.73	46.28
FeO	14.47	15.53	13.90	14.89	15.53	15.38	15.45	13.22	13.66	14.53
MnO	0.11	0.12	0.08	0.15	0.13	0.13	0.20	0.10	--	0.09
MgO	14.28	13.31	14.86	13.85	13.64	13.78	14.00	15.56	14.66	13.90
CaO	--	--	--	0.07	--	0.11	0.11	0.09	0.08	0.11
Na <sub>2</sub> O	n/a	n/a	n/a	n/a	n/a	n/a	n/a	n/a	n/a	n/a
K <sub>2</sub> O	n/a	n/a	n/a	n/a	n/a	n/a	n/a	n/a	n/a	n/a
NiO	--	--	0.09	--	--	--	0.13	--	0.09	--
Total	99.29	99.48	99.15	99.12	100.13	99.07	99.11	99.33	99.84	99.22
Grain	1	1	1	2	2	2	4	7a	7a	7b
Oxygens	4	4	4	4	4	4	4	4	4	4
Si <sup>4+</sup>	--	--	0.015	--	--	--	0.013	--	--	--
Ti <sup>4+</sup>	--	--	--	--	--	--	--	--	--	--
Al <sup>3+</sup>	0.897	0.913	0.890	0.882	0.887	0.844	0.833	0.944	0.745	0.872
Cr <sup>3+</sup>	1.090	1.081	1.072	1.104	1.103	1.132	1.115	1.031	1.234	1.119
Fe <sup>2+</sup>	0.368	0.396	0.352	0.381	0.394	0.397	0.398	0.331	0.352	0.372
Mn <sup>2+</sup>	0.003	0.003	0.002	0.004	0.003	0.003	0.005	0.002	--	0.002
Mg <sup>2+</sup>	0.647	0.604	0.671	0.632	0.617	0.633	0.642	0.695	0.672	0.634
Ca <sup>2+</sup>	--	--	--	0.002	--	0.004	0.004	0.003	0.003	0.004
Na <sup>+</sup>	n/a	n/a	n/a	n/a	n/a	n/a	n/a	n/a	n/a	n/a
K <sup>+</sup>	n/a	n/a	n/a	n/a	n/a	n/a	n/a	n/a	n/a	n/a
Ni <sup>2+</sup>	--	--	0.002	--	--	--	0.003	--	0.002	--
Total	3.006	3.001	3.004	3.006	3.005	3.012	3.013	3.010	3.009	3.004
Mg#	0.64	0.60	0.66	0.62	0.61	0.61	0.62	0.68	0.66	0.63
Cr#	0.55	0.54	0.55	0.56	0.55	0.57	0.57	0.52	0.62	0.56

## CHAPTER 6

### GEOTHERMOBAROMETRY

---

#### 6.1 GEOTHERMOBAROMETERS USED

Equilibrium temperatures and pressures for mantle xenoliths have been calculated for five samples (xenolith 89490B could not be used as it does not contain any of the required mineral pairs used for geothermobarometry). Geothermobarometers calibrated for ultramafic and mafic compositions of rocks for high pressures and temperatures expected in the mantle were used. The following geothermobarometers have been applied to the Tuwawi xenoliths: two-pyroxene geothermometer of Brey and Köhler (1990) (BK) and Finnerty and Boyd (1987) (FB), olivine-garnet geothermometer of O'Neill and Wood (1979) (OW), olivine-spinel geothermometer of Roeder et al. (1979), clinopyroxene-garnet geothermometer of Ellis and Green (1979) (EG), garnet-orthopyroxene geobarometer of Brey and Köhler (1990) (BK) and MacGregor (1974) (MG). In general, errors for thermobarometry are  $\pm 25$  °C and  $\pm 2$  kbar (Winter, 2001).

All values of pressure and temperature were calculated using the TP92 program. The TP92 program was revised to run on Mac by Andrew Freeman and Norm Pearson from the original FORTRAN 4 version by Doug Smith. TP92 calculates equilibration pressure and temperatures in rocks consisting of two or more of the following phases: olivine, orthopyroxene, clinopyroxene, garnet and spinel. The program reads original microprobe data from an input data file, and corresponding geothermometers and geobarometers are applied, depending on which phases are present in the sample.

The two-pyroxene geothermometer of Brey and Köhler (1990) is based on the exchange of the enstatite component between orthopyroxene and clinopyroxene. Experiments were carried out on primitive natural lherzolitic compositions in the pressure-temperature ranges of 10-60 kb and 900-1400 °C (Brey et al., 1990). The Finnerty and Boyd (1987)

geothermometer is based off of the reverse reaction of the exchange of Ca between orthopyroxene and clinopyroxene. This thermometer is applicable to garnet lherzolites (Finnerty and Boyd, 1984).

The geothermometer of O'Neill and Wood (1979) is based on the Fe-Mg partitioning between garnet and olivine, and is applicable to rocks with Mg-rich olivine-garnet assemblages within the temperature range 90-1400 ° C and pressures up to 60 kb.

The geothermometer of Ellis and Green (1979) is based on the Fe-Mg exchange between coexisting garnet and clinopyroxene. This exchange has been found to be dependant on the Ca-content of the two phases rather than the  $Mg/(Fe+Mg)$ . Its application is to rocks of basaltic composition as well as those with compositions lying within the CaO-FeO-MgO- $Al_2O_3$ -SiO<sub>2</sub> (CFMAS) system, that have crystallized garnet and clinopyroxene within the pressure-temperature range of 24-30 kb and 750-1300 °C (Ellis and Green, 1979).

The geothermometer of Roeder et al. (1979) is based off of the Mg-Fe exchange between coexisting olivine and spinel. Experiments were conducted within the range of temperature 500-800 °C, and are applicable to basic plutonic rocks (Roeder et al., 1979).

The geobarometers used are both based on the solubility of  $Al_2O_3$  in orthopyroxene coexisting with garnet. Brey and Köhler (1990) carried out experiments on primitive natural lherzolithic compositions in the pressure-temperature ranges of 28-60 kb and 900-1400 °C. The geobarometer of MacGregor (1974) works in the temperature and pressure range of 900-1600 ° C and 5-40 kbar and is applicable to spinel and garnet peridotites (MacGregor, 1974).

## **6.2 METHODOLOGY OF P-T ESTIMATES**

If the microprobe analyses of minerals in each sample showed low variance in chemical compositions they were averaged by oxide wt%. The number of averaged analyses varies from 2 to 19 (Appendix II). For spinel, which exhibited heterogeneous chemical compositions (sample 89487), analyses were not averaged. In sample 89497, all except one spinel core analysis were averaged with 2 or 3 chemical analyses, whereas all rims were left

as is. Separate temperature and pressure calculations were then conducted for each spinel analysis (averaged and not). Results are presented in Table 7. Since various geothermometers measure temperatures for diffusion closure for different equilibria (i.e. Mg-Fe exchange between olivine and spinel, or the Ca-Mg exchange between orthopyroxene and clinopyroxene), the geothermometers do not yield the same temperatures for a given sample. Therefore a large spread of pressures and temperatures was calculated for each sample (Fig. 6). It was decided to use the geothermobarometers applied in literature on kimberlites from adjacent areas, as data from neighboring kimberlites were needed to compare to the results from the Tuwawi kimberlite. There is presently only one other kimberlite occurrence on Brodeur Peninsula (Freightrain), but no comparable data is available for it, thus all comparisons are with kimberlites on Somerset Island (Nikos kimberlite (Schmidberger and Francis, 1998), Ham kimberlite (Jago and Mitchell, 1987), and Batty Bay kimberlite complex (Kjarsgaard and Peterson, 1992)).

Temperature and pressure estimates depend upon each other; therefore P-T estimates in Table 7 are given in pairs. For samples containing olivine-orthopyroxene-clinopyroxene-garnet (89490, 89494, 89481, 89497), temperatures were calculated using the 2-pyroxene thermometers of BK and FB, and pressures using the orthopyroxene-garnet barometers of BK and MG. T-P pairs were also calculated using the olivine-garnet thermometer of OW and orthopyroxene-garnet MG barometer. Some of the above samples (89487, 89497) also contained spinel. For these samples, olivine-spinel temperatures were additionally calculated using the Roeder thermometer. Since spinel is zoned and shows inter-granular heterogeneity, the Roeder temperatures vary from 670 to 859 °C for sample 89487, and 890 to 1007 °C for sample 89497. Due to the different bulk composition of sample 89481 (clinopyroxenite), the EG thermometer, calibrated for mafic compositions, was applied for a given range of pressures 20-60 kb. Where garnet was absent (89487), pressures could not be calculated. In this case only the olivine-spinel thermometer can be used to estimate temperatures as it is not dependent on pressure.

Table 7. Equilibrium temperature and pressure estimates for the Tuwawi mantle xenoliths														
Sample	Mineralogy	Texture	Opx-Cpx T(C), Opx-Gar P (kb)						Ol-Gar T(C), Opx-Gar P (kb)		Cpx-Gar T(C),			Spl-Ol
			BK		FB-MG		BK-MG		OW-MG		EG			Roeder
			T (oC)	P (kb)	T (oC)	P (kb)	T (oC)	P (kb)	T (oC)	P (kb)	20kb	40kb	60kb	T (oC)
89490	GarOpxCpxOl	M-P	1199	53.3	1140	53.8	1206	58.1	1144	54.0				
89494	GarOpxCpxOl	P	1303	70.4	1209	60	1288	65.3	1276	62.7				
89497	GarOpxCpxOlSpl	C	666	25	627	22	637	22.7	843	36.9				
Grain 1&3	Cr-rich core													970
1	Cr-rich rim													946
3	Cr-rich rim													1007
2&9	Al-rich core													956
8	core													964
8	rim													958
7	Fe-rich core													890
7	Fe-rich rim													902
89487	OpxCpxOlSpl	C												
Grain 1	Al-poor rim													770
1	core													775
1	core													670
1	rim													779
2a	core													702
2b	core													730
2c	core													751
4	rim													760
7a	Al-rich core													849
7a	Cr-rich rim													859
7b	rim													738
89481	GarOpxCpx		1257	84.1	1103	55.7	1216	63.4			1047	1127	1206	

**Table 7.** Equilibrium temperature and pressure estimates for the Tuwawi kimberlite. Where Gar=garnet, Opx=orthopyroxene, Cpx=clinopyroxene, Ol=olivine, Spl=spinel, M-P=mosaic-porphyroclastic, P=porphyroclastic, C=coarse, BK= Brey and Köhler (1990), FB=Finnerty and Boyd (1987) geothermometer, MG=MacGregor (1974) geobarometer, OW=O'Neill and Wood (1979), EG=Ellis and Green (1979), and Roeder=Roeder et al. (1979).

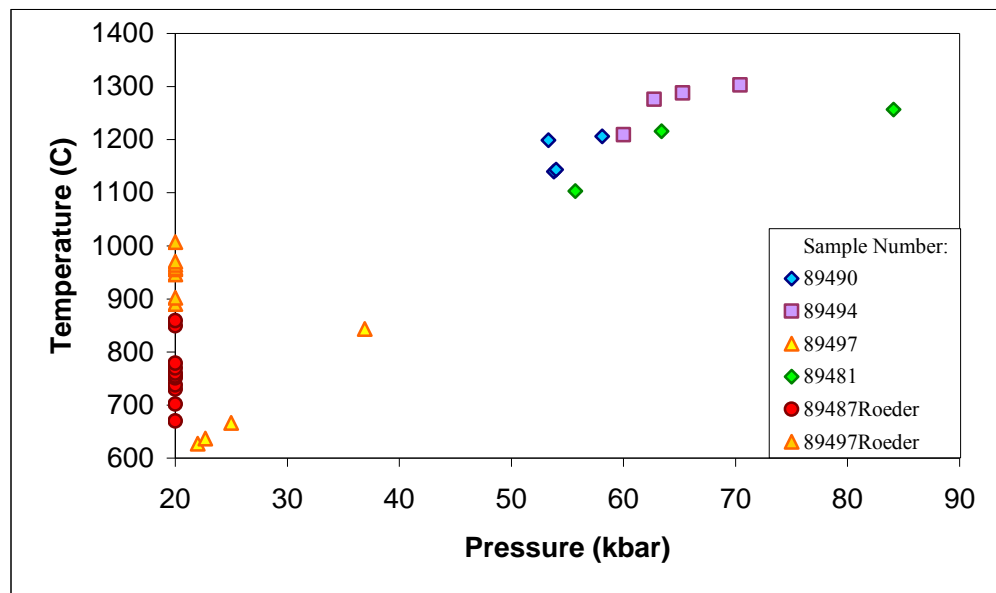
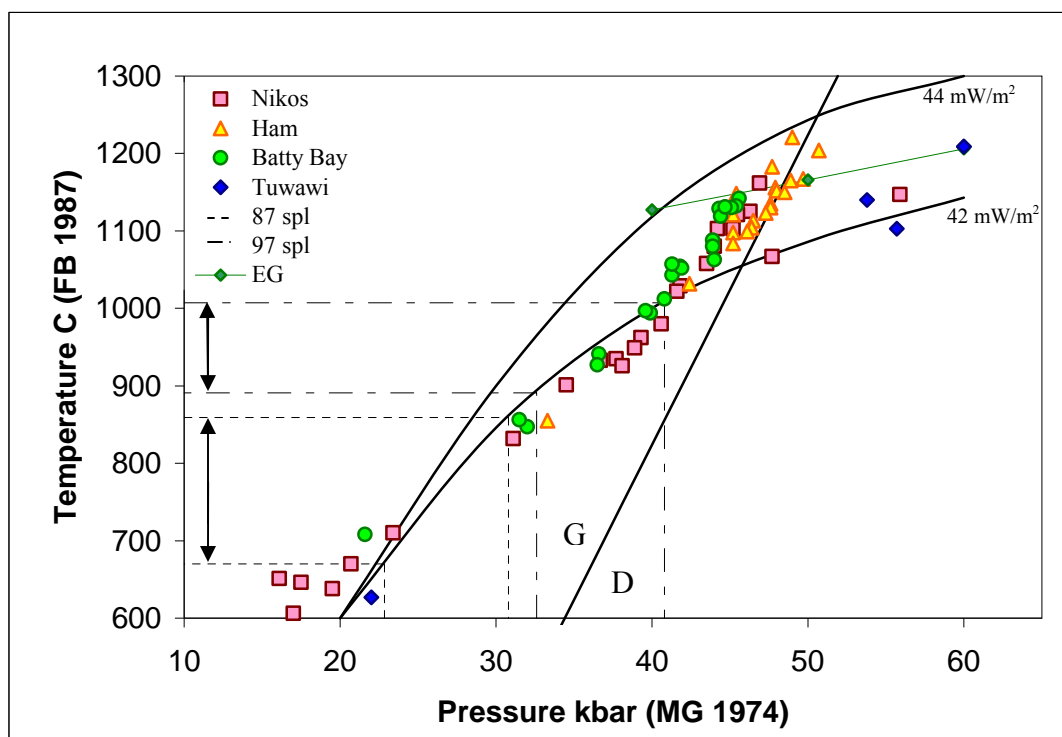


**Figure 6.** Variation in equilibrium pressure and temperature estimates of the Tuwawi mantle xenoliths in using different geothermobarometric methods (See Table 7.1).

### 6.3 RESULTS AND COMPARISON WITH LITERATURE DATA

Results of thermobarometric analysis allowed for comparison of the thermal state of the Tuwawi mantle, at the time of the kimberlite emplacement, with the corresponding data from adjacent kimberlites. As mentioned above, these kimberlites include the Batty Bay kimberlite complex (Kjarsgaard and Peterson, 1992), the Nikos kimberlite (Schmidberger and Francis, 1998), and the Ham kimberlite (Jago and Mitchell, 1987). Like Baffin Island, Somerset Island lies within the Rae Domain consisting of Archean basement (Eyles and Miall, 2007). Kimberlite occurrences on both islands were emplaced during the Cretaceous (Heaman, 1989; Zhao et al., 1997).

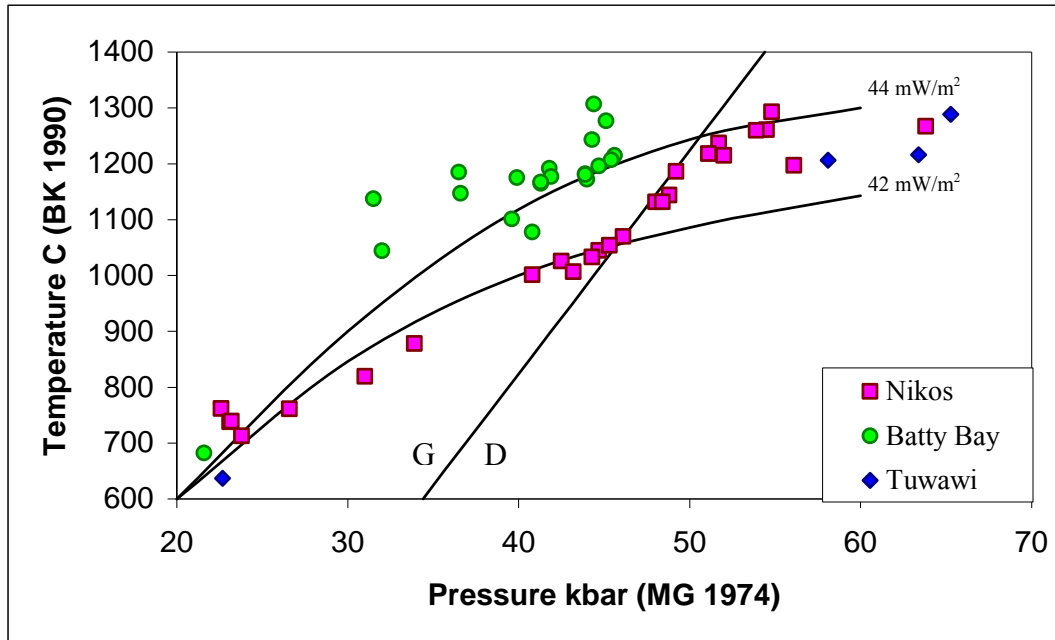
On the FB temperature-MG pressure diagram, xenoliths from Tuwawi show T-P values of 1140 °C-53.8 kb, 1209 °C-60 kb, 627 °C-22 kb and 1103 °C-55.7 kb. In comparison to the Somerset Island xenoliths, deformed peridotite and clinopyroxenite xenoliths of Tuwawi plot at higher pressures, and higher temperatures compared to the majority of Somerset data (Fig. 7). The coarse peridotite of Tuwawi plots within the same area as coarse samples from the Nikos and Batty Bay kimberlites. The Tuwawi xenoliths plot in the vicinity of the 42 mW/m<sup>2</sup> geotherm of Gurney and Harte (1980). This geotherm was used to estimate pressure ranges for samples 89487 and 89497 corresponding to the olivine-spinel temperatures found using the Roeder thermometer. It is to be noted that these are rough estimates calculated to only give perspective on the possible P-T location of these samples. This graphical method was also used to find an approximate P-T location for the clinopyroxenite sample (89481) using temperatures from the Ellis and Green (1979) thermometer for various pressures. This trend of data does not cross the 42 mW/m<sup>2</sup> geotherm thus intersection with the 44 mW/m<sup>2</sup> geotherm was used and a P-T location of 1131 °C, 41 kb was estimated.



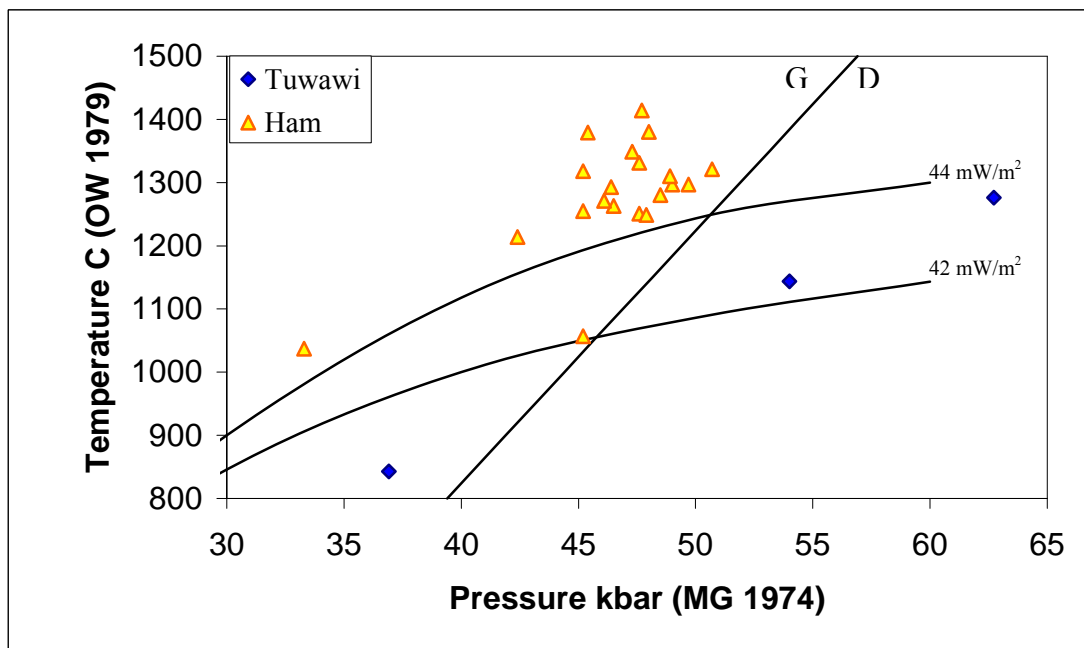
**Figure 7.** Equilibrium temperature and pressure for the Tuwawi mantle xenoliths as compared to Nikos data (Schmidberger and Francis, 1998), Ham data (Jago and Mitchell, 1987), and Batty Bay Complex data (Kjarsgaard and Peterson, 1992) of Somerset Island. FB – Finnerty and Boyd (1987) geothermometer, MG – MacGregor (1974) geobarometer, EG – Ellis and Green (1979) thermometer. Diamond-graphite equilibrium line from Kennedy and Kennedy (1976), D=diamond, G=graphite. The theoretical 44 mW/m<sup>2</sup> and 42 mW/m<sup>2</sup> geotherms are from Gurney and Harte (1980). 87 spl, 97 spl – olivine-spinel temperatures of Roeder et al. (1979) for samples 89487 and 89497. Dashed lines project approximations of the maximum and minimum pressures along the 42 mW/m<sup>2</sup> geotherm corresponding to the max and min olivine-spinel temperatures.

Figure 8 illustrates data calculated using the BK thermometer-MG barometer. Data from the Nikos and Batty Bay kimberlites are plotted for comparison, and also show lower pressures and temperatures than the data from Tuwawi (1288 °C - 65.3 kb, 1216 °C - 63.4 kb, 1206 °C - 58.1 kb, and 637 °C - 22.7 kb). In this case the Tuwawi data plots between the 44 and 42 mW/m<sup>2</sup> geotherms along, or close to, what could be estimated as a 43 mW/m<sup>2</sup> geotherm. Figure 9 illustrates the OW thermometer-MG barometer data of Tuwawi in comparison to that of the Ham kimberlite. Samples 89490, 89494 and 89497 are represented and give P-T locations of 54 kb - 1144 °C, 62.7 kb - 1276 °C, and 36.9 kb - 843 °C respectively. The majority of the Ham data plots at higher temperatures and lower pressures than that of Tuwawi, and follows a geothermal trend just above 44 mW/m<sup>2</sup>. The Tuwawi data does not follow a curved modeled geothermal trend; rather an almost linear trend is present.





**Figure 8.** Equilibrium temperature and pressure for the Tuwawi mantle xenoliths as compared to Nikos data (Schmidberger and Francis, 1998), and Batty Bay Complex data (Kjarsgaard and Peterson, 1992) of Somerset Island. Theoretical geotherms and diamond-graphite transition as per Figure 7.



**Figure 9.** Equilibrium temperature and pressure for the Tuwawi mantle xenoliths as compared to Ham data (Jago and Mitchell, 1987) of Somerset Island. OW – O'Neill and Wood (1979) thermometer, MG – MacGregor (1974) barometer. Theoretical geotherms and diamond-graphite transition as per Figure 7.

Correlation between pressures and temperatures of equilibrium and the mineralogy and textures of the rocks was examined. Deformed peridotites and clinopyroxenite samples show similar temperatures and pressures, which are much higher than those of the coarse peridotites. The porphyroclastic sample (89494) consistently shows higher P-T values than those of the mosaic-porphyroclastic sample (89490). Samples containing spinel also show much lower temperatures and pressures than those without spinel but containing garnet. This matches the pattern expected for peridotites of different depth facies (Winter, 2001). Though no pressure could be calculated for sample 89487, the whole range of calculated temperatures (670-859 °C) falls well below those of the deformed peridotites and the clinopyroxenite. The Tuwawi data corresponds with a 42 mW/m<sup>2</sup> geotherm for the most part. The two deformed peridotite samples and the pyroxenite sample plot well into the diamond stability field, as defined by Kennedy and Kennedy (1976), whereas coarse peridotites plot within the graphite stability field (Fig. 8 and Fig. 9).

## CHAPTER 7

### DIAMOND POTENTIAL OF THE TUWAWI KIMBERLITE

---

Determining the position of the geotherm is said to be the most important factor in determining the likelihood of a kimberlite pipe to contain diamonds (Griffin and Ryan, 1995). If the geotherm is high, diamonds become stable at greater depths, and the diamond potential of the hot mantle is low. If the geotherm is inflected at shallow depths it will not enter the diamond stability field within the lithosphere, and thus will not encounter diamonds. Therefore it must be determined to what geotherm the Tuwawi xenoliths correspond the closest. As has been discussed above, the Tuwawi data seems to correspond to a continental geotherm of  $42 \text{ mW/m}^2$ . This is hotter than is normally preferred for a high diamond potential. Preferred geotherms correspond to those of  $38\text{-}40 \text{ mW/m}^2$  or lower (Griffin and Ryan, 1995).

It has been proposed by Boyd and Gurney (1986), that there is a correlation between textural type of xenoliths and their estimated pressure-temperatures of equilibrium. High-temperature, deformed peridotite xenoliths are found to give equilibrium pressure-temperature estimates which deviate from the proposed geotherm towards higher temperatures, whereas low-temperature, coarse peridotites plot close to the proposed geotherm (Boyd and Gurney 1986). This model accommodates for the slight deviation of the high-temperature samples from the  $42 \text{ mW/m}^2$  seen in the Tuwawi xenoliths. Although, it must be noted that due to the very small number of samples analyzed in this paper, correlation to a geotherm is highly speculative and a larger suite of samples from the area need to be examined before a definite geothermal gradient can be assigned. In any case, the mantle xenolith samples from the Tuwawi kimberlite can give some insight into the state of the mantle below northwestern Baffin Island, and the prospects for diamond potential. The inflection point described above is thought to represent the boundary between the lithosphere and the asthenosphere where there is a distinction between physical and possibly chemical

properties (Boyd and Gurney 1986). With this, and the common belief that diamonds come from the lithosphere rather than the asthenosphere (Boyd and Gurney 1986), a P-T range can be constrained corresponding to the 'diamond window'. This diamond window is the stability field of diamond within the lithosphere and is defined by temperatures between the base of the unmodified lithosphere and the intersection of the geotherm with the diamond-graphite equilibrium line (Griffin and Ryan, 1995). If a geotherm of  $42 \text{ mW/m}^2$  is used for the Tuvawu samples, a temperature range of  $1050^\circ\text{C}$  to  $<1100^\circ\text{C}$  corresponds to the diamond window.

In addition to the thermal state of the mantle and the depth to the lithosphere-asthenosphere boundary, the diamond potential of a pipe is controlled by near surface processes. These include the geology of the kimberlite pipe and the post-emplacement erosion. Generally, diamond potential of volcanoclastic kimberlite (kimberlite of the diatreme and crater facies) is higher than that of the hypabyssal kimberlite (Kopylova, personal communication, 2009). This is related to the enrichment of diamond, and all other mantle components, due to elutriation of ash during volcanic eruptions. There is also the common belief that crater facies rocks represent a significant source of diamond, as is evident from the Orapa deposit in Botswana (Mitchell, 1991). A high diamond potential of the Tuvawu kimberlite is favoured by the presence of volcanoclastic kimberlite.

Exposure of the Tuvawu kimberlite is in the crater facies, as can be concluded from the presence of volcanoclastic kimberlite. The existence of the crater facies implies that a low level of erosion has occurred since emplacement. It has been inferred that emplacement of the Tuvawu kimberlite occurred during the Cretaceous. Since only sediments deposited up to the Middle Silurian still remain in this area (Trettin, 1969), it can be assumed that surface processes kept the surface stratigraphy of the area to a minimum between the Middle Silurian and the Cretaceous for such little erosion of the kimberlite to have occurred. The maximum level of erosion is estimated to be  $\sim 400\text{m}$ - $500\text{m}$  based on the maximum depths where volcanoclastic kimberlites of the crater facies are found at Lac de Gras (Field and Scott Smith, 1999).

In conclusion, several positive and negative factors for the diamond potential of the Tuwawi kimberlite were found. Positive factors include an exposure in the crater facies, and equilibrium pressures and temperatures plotting well into the diamond stability field for three of the six mantle xenoliths sampled. Negative factors include a hotter than desired geotherm of  $\sim 42 \text{ mW/m}^2$ , and a narrow “diamond window”. As this paper should be considered as preliminary, a more in-depth study is recommended, using a much larger suite of samples from the Tuwawi kimberlite to better constrain the geothermal gradient within the mantle and the “diamond window”.

## REFERENCES

---

- Berman, R. G., Sanborn-Barrie, M., Stern, R. A., Carson, C. J., 2005, Tectonometamorphism at ca. 2.35 and 1.85 Ga in the Rae Domain, Western Churchill Province, Nunavut, Canada: Insights from Structural, Metamorphic and in situ Geochronological Analysis of the southwestern Committee Bay Belt, *The Canadian Mineralogist*, v. 43, p. 409-442.
- Boyd, F. R. and Gurney, J. J., 1986, Diamonds and the African Lithosphere, *Science*, v. 232, p. 472-477.
- Brey, G. P. and Kohler, T., 1990, Geothermobarometry in Four-phase Lherzolites II. New Thermobarometers, and Practical Assessment of Existing Thermobarometers, *Journal of Petrology*, v. 31, n. 6, p. 1353-1378.
- Brey, G. P., Kohler, T. and Nickel, K.G., 1990, Geothermobarometry in Four-phase Lherzolites I. Experimental Results from 10 to 60 kb, *Journal of Petrology*, v. 31, n. 6, p. 1313-1352.
- Dawson, J. B. and Stephens, W. E., 1975, Statistical Classification of Garnets from Kimberlite and Associated Xenoliths, *Journal of Geology*, v. 83, p. 589-607.
- Ellis, D. J. and Green, D. H., 1979, An Experimental Study of the Effect of Ca Upon Garnet-Clinopyroxene Fe-Mg Exchange Equilibria, *Contributions to Mineralogy and Petrology*, v. 71, p. 13-22.
- Eyles, N. and Miall, A., editors, 2007, *Canada Rocks: The Geologic Journey*, Fitzhenry and Whiteside Ltd., Ontario, 512 p.
- Field, M. and Scott Smith, B. H., 1999, Contrasting geology and near-surface emplacement of kimberlite pipes in southern Africa and Canada, In: Gurney, J. J., Gurney, J. L., Pascoe, M. D., and Richardson, S. H., editors, *Proceedings of the 7th International Kimberlite Conference vol. 1*, Red Roof Design, Cape Town, p. 214-237.
- Finnerty, A. A. and Boyd, F. R., 1984, Evaluation of thermobarometers for garnet peridotites, *Geochimica et Cosmochimica Acta*, v. 48, p. 15-27.
- Finnerty, A. A. and Boyd, F. R., 1987, Thermobarometry for garnet peridotites: basis for the determination of thermal and compositional structure of the upper mantle, In: Nixon, P. H., editor, *Mantle Xenoliths*, John Wiley and Sons Ltd., p. 381-402.
- Frisch, T., 1982, Precambrian Geology of the Prince Albert Hills, Western Melville Peninsula, Northwest Territories, *Geological Survey of Canada, Bulletin* 346

- Griffin, W. L. and Ryan, C. G., 1995, Trace elements in indicator minerals: area selection and target evaluation in diamond exploration, *Journal of Geochemical Exploration*, v. 53, p. 311-337.
- Gurney, J. J. and Harte, B., 1980, Chemical Variations in Upper Mantle Nodules from Southern African Kimberlites, *Philosophical Transactions of the Royal Society of London, Series A*, v. 297, n. 1431, p. 273-293.
- Harte, B., 1977, Rock Nomenclature with particular relation to deformation and recrystallization textures in olivine-bearing xenoliths, *Journal of Geology*, v. 85, p. 279-288.
- Harte, B., 1978, Kimberlite Nodules, Upper Mantle Petrology, and Geotherms. *Philosophical Transactions of the Royal Society of London, Series A*, v. 288, no. 1355, p. 487-500.
- Heaman, L. H., 1989, The nature of the subcontinental mantle from Sr–Nd–Pb isotopic studies on kimberlite perovskite, *Earth Planetary Science Letters* v. 92, p. 323–334.
- Jackson, G. D., and Berman, R. G., 2000, Precambrian metamorphic and tectonic evolution of Northern Baffin Island, Nunavut, Canada, *The Canadian Mineralogist* v. 38, p. 399-421.
- Jago, B. C., Davis, D., and Derbuch, H., 2002, Diamonds on the Brodeur Peninsula – A new kimberlite province in Nunavut, Canada, *CIM Bulletin*, v. 95, p. 72-78.
- Jago, B. C., and Mitchell, R. H., 1987, Ultrabasic xenoliths from the Ham kimberlite, Somerset Island, Northwest Territories, *Canadian Mineralogist*, v. 25, p. 515-525.
- Kennedy, C. S. and Kennedy G. C., 1976, The equilibrium boundary between graphite and diamond, *Journal of Geophysical Research*, v. 81, n. B14, p. 2467-2470
- Kjarsgaard, B.A, and Peterson, T.D. 1992. Kimberlite-derived ultramafic xenoliths from the diamond stability field: a new Cretaceous geotherm for Somerset Island, Northwest Territories; in *Current Research, Part B; Geological Survey of Canada, Paper 92-1B*, p. 1-6.
- Kopylova, M., 2009, Personal Communication.
- MacGregor, I. D., 1974, The System MgO-Al<sub>2</sub>O<sub>3</sub>-SiO<sub>2</sub>: Solubility of Al<sub>2</sub>O<sub>3</sub> in Enstatite for Spinel and Garnet Peridotite Compositions, *American Mineralogist*, v. 59, p. 110-119.
- Mitchell, R. H., 1991, Kimberlites and Lamproites: Primary Sources of Diamond, *Geoscience Canada*, v. 18, n. 1, p. 1-16.

- Nicholas, A., Bouchez, J. L., Doudier, F., and Mercier, J. C., 1971 Textures, structures and fabrics due to solid state flow in some European lherzolites, *Tectonophysics*, v. 12, p. 55-86.
- Nimis, P. and Taylor, W. R., 2000, Single clinopyroxene thermobarometry for garnet peridotites. Part I. Calibration and testing of a Cr-in-Cpx barometer and an enstatite-in-Cpx thermometer. *Contributions to Mineralogical Petrology*, v. 139, p. 541-554.
- Nixon, P. H., Rogers, N. W., Gibson, I. L., and Grey, A., 1981, Depleted and Fertile Mantle Xenoliths from Southern African Kimberlites, *Annual Review of Earth and Planetary Sciences*, v. 9, p. 285-309.
- O'Neill, H. St.C. and Wood, B. J., 1979, An Experimental Study of Fe-Mg Partitioning Between Garnet and Olivine and Its Calibration as a Geothermometer, *Contributions to Mineralogy and Petrology*, v. 70, p. 59-70.
- Pouchou, J. L. and Pichoir, F., 1985, PAP  $\phi(\rho Z)$  procedure for improved quantitative microanalysis. In: Armstrong, J.L., Editor, *Microbeam Analysis*, San Francisco Press Inc, San Francisco, p. 104–106.
- Ritcey, B. D., 2007, Maps of Brodeur Property geology and property location (unpublished).
- Ritcey, B. D., 2008, Introductory information on Brodeur Property, Qikiqtani Region (Baffin Island), Nunavut (unpublished).
- Roeder, P. L., Campbell, I. H., and Jamieson, H. E., 1979, A Re-Evaluation of the Olivine-Spinel Geothermometer, *Contributions to Mineralogy and Petrology*, v. 68, p. 325-334.
- Schmidberger, S. S. and Francis, D., 1999, Nature of the mantle roots beneath the North American craton: mantle xenolith evidence from Somerset Island kimberlites, *Lithos*, v. 48, p.195-216.
- Scott Smith, B., 1996, Kimberlites, In: Mitchell, R. H., editor, *Undersaturated Alkaline Rocks: Mineralogy, Petrogenesis and Economic Potential*, Mineralogical Association of Canada, Ontario, 312 pages.
- Trettin, H. P., 1969, Lower Palaeozoic Sediments of Northwestern Baffin Island, District of Franklin, Geological Survey of Canada, Bulletin 157
- Trettin, H. P., 1991, Geology of the Innuitian Orogen and the Arctic Platform of Canada and Greenland, Geological Survey of Canada, *Geology of Canada*, n. 3, v. E.
- Winter, J. D., editor, 2001, *An Introduction to Igneous and Metamorphic Petrology*, Prentice Hall, New Jersey, 697 p.



Zhao, D., Essene, E. J., Zhang, Y., Hall, C. M., and Wang, L., 1997, Newly Discovered Kimberlites and Mantle Xenoliths from Somerset Island and Brodeur Peninsula, Canada: Pressure, Temperature, Oxygen Fugacity, Volatile Content and Age, NWT Geology Division, Department of Indian and Northern Affairs, p. 1-105.

## APPENDIX I

### THIN SECTION DESCRIPTIONS

---

#### A. MANTLE XENOLITHS:

Sample: **89490**

Thin Section: 89490A

Rock Name: Garnet Lherzolite

Texture: Mosaic-porphyroclastic

Primary Minerals:

- 70% Olivine – Grains occur 5% as porphyroclasts and 65% as neoblasts. Porphyroclast grains occur as anhedral crystals, ranging in size from approximately 1.1x1.2 mm to 0.32x0.16 mm. Grains show undulose extinction. Neoblast grains occur as subhedral to anhedral crystals and form in sizes ranging from 1.1x0.8 mm to 10  $\mu$ m. They show low birefringence colours of grey/white to yellow with a few grains showing colours up to second order blue.
- 15% Orthopyroxene – Grains occur 12% as porphyroclasts and 3% as neoblasts. Porphyroclasts occur as subhedral to anhedral crystals with raggedy edges. Grains range in size from 2.4x1.5 mm to 0.16x0.16 mm. Most grains show signs of partial melting in the form of small inclusions around their rims. There are some crystals that have been entirely recrystallized. Grains show undulose extinction and are present in both basal sections with two cleavages at approximately 90 degrees, as well as in longitudinal sections showing one good cleavage. The majority of grains are fractured. Neoblasts occur as subhedral to anhedral equant grains ranging in size from 0.05 mm to 10  $\mu$ m. They are only found around and between porphyroclasts.
- 10% Clinopyroxene - Grains occur 14% as porphyroclasts and 1% as neoblasts. Porphyroclasts occur as subhedral to anhedral crystals with raggedy edges. Grains

range in size from 2.4x1.5 mm to 0.16x0.16 mm. Most grains show signs of partial melting in the form of small inclusions around their rims. Grains show undulose extinction and are present in both basal sections with two cleavages at approximately 90 degrees, as well as in longitudinal sections showing one good cleavage. The majority of grains are fractured. Neoblasts occur as subhedral to anhedral equant grains ranging in size from 0.05 mm to 10  $\mu$ m, and remain in close proximity to porphyroclasts. Grains show abnormally low birefringence, and so can only be differentiated from orthopyroxene by an angular extinction.

- 5% Garnet - Grains occur as subhedral to euhedral, equant crystals ranging in size from 4.2x4.5 mm to 3.4x3.2 mm. All grains have kelyphitic rims with varying thickness proportional to the size of the garnet grain; larger grains have thicker rims. All grains are highly fractured. Largest grain has an inclusion of a euhedral, tabular mineral with low birefringence colour and ~20 degree extinction – olivine(?)

#### Secondary Minerals:

- Calcite - vein across largest garnet grain which then extends out past kelyphitic rim and disperses into interstices of adjacent neoblasts. There is also some interstitial calcite alteration in inclusion rims of orthopyroxene grains.
- Kelyphite – cryptocrystalline, low birefringence colours of grey/white. Crystals form in fibrous radiating fan patterns. The extinction fans across grains. The grain size coarsens slightly moving away from garnet grain boundary.

#### Thin Section: 89490B

Note: Thin section seems to have two xenoliths of different composition and texture separated by carbonaceous material with anhedral olivine grains, likely kimberlite (?). Xenolith A is the same xenolith as in thin section 89490A.

#### **Xenolith A:**

Rock Name: Garnet Lherzolite

Texture: Mosaic-Porphyroclastic

Primary Minerals:

- 70% Olivine – Grains occur as almost strictly neoblasts, except for one visible porphyroclastic grain showing undulose extinction. The porphyroclast grain is anhedral, and 1.6x0.96 mm in size. Neoblast grains occur as equant, anhedral crystals, ranging in size from 10 µm to 0.88x0.8mm.
- 15% Orthopyroxene – Porphyroclast grains occur as subhedral to anhedral, equant and tabular crystals, ranging in size from 1.7x1 mm to 0.2x0.08 mm. Neoblasts occur as anhedral crystals ranging in size up to 100x60 µm. Grains show a fluidal texture, forming lenticles between porphyroclasts. Grains are present in both basal sections with two cleavages at ~90 degrees, and longitudinal sections with one cleavage. There are also some grains that do not show any cleavage. Some grains have very faint pink pleochroism.
- 14% Clinopyroxene – Grains are euhedral to subhedral, ranging in size from 0.88x1 mm to 0.24x0.32 mm, and showing interference colours up to second order blue. Some grains show faint pale brown or green pleochroism. Only longitudinal sections are present with one cleavage. Grains show an angular extinction of ~45 degrees and some have undulose extinction as well. Partial melting inclusions are present around grain edges, and some grains are completely included.
- 1% Garnet – There is half a grain of garnet along one edge of the sample. It is approximately 1.2x3.1mm in size with a kelyphitic rim.

Secondary Minerals:

- Kelyphite – cryptocrystalline, fines towards garnet grain boundary, fibrous radiating texture (fans).
- Serpentine and phlogopite (?) alteration around xenolith edge adjacent to kimberlite (?)
- Mosaic texture is lost moving out to edge of xenolith as serpentine and phlogopite alteration overprints grains.

**Xenolith B:**

Rock Name: Dunite

Texture: Porphyroclastic

**Primary Minerals:**

- 97% Olivine – 94% occurring as porphyroclasts, 3% as neoblasts. Porphyroclast grains occur as subhedral to anhedral crystals, ranging in size from 5.6x6.9 mm to 0.64x0.4 mm. Grains are fractured with ragged edges, and most show undulose extinction. The larger grains at the edges of the sample show inclusions following fracture patterns. Neoblast grains occur as anhedral crystals, ranging in size up to 0.48x0.76 mm. Interference colours are up to second order blue/purple.
- ~3% Orthopyroxene – Grains occur as subhedral to anhedral crystals, ranging in size from 1.2x0.56 mm to 0.24x0.28 mm. Only longitudinal sections are present showing one cleavage. Grains are highly fractured, and show undulose extinction.

**Secondary Minerals:**

- Serpentine alteration in fractures of olivine and of orthopyroxene grains.
- Alteration mineral present in fractures and interstices of olivine and orthopyroxene showing high interference colours up to second order blue and green, and form triangular crystals – most likely talc.

Sample: **89494**

Thin Section: 89494

Rock Name: Garnet Lherzolite

Texture: Porphyroclastic

**Primary Minerals:**

- 85% Olivine – Grains occur 18% as porphyroclasts and 67% as neoblasts. Porphyroclasts occur as anhedral to subhedral crystals ranging in size from 1.2x2.3 mm to 0.36x0.16

- mm. The larger grains are more fractured and altered to serpentine (and/or phlogopite (?)). Neoblasts occur as anhedral equant crystals ranging in size up to 0.96x0.56 mm. Grains show interference colours up to second order blue.
- 8% Orthopyroxene – Grains occur as euhedral to subhedral crystals with ragged boundaries. Grains range in size from 0.96x1.6 mm to 0.28x0.2 mm. Most grains show inclusions from partial melting around edges. Grains are present in both basal sections with two cleavages at approximately 90 degrees, as well as in longitudinal sections showing one good cleavage.
- 5% Clinopyroxene – Grains occur as euhedral to subhedral crystals, ranging in size from 0.64x0.48 mm to 0.2x0.28 mm. Birefringence colours are first order greys, but a faint cleavage is visible showing angular extinction. Most grains show inclusions from partial melting around edges.
- 2% Garnet - Grains occur as euhedral crystals with kelyphitic rims, ranging in size from 3.3x2.7 mm to 1.4x0.8 mm. Most garnet grains have been almost completely replaced by Kelyphite.

Secondary minerals:

- Serpentine – in fractures and interstices of olivine.
- Phlogopite/ Talc (?) – interference colours up to second order green and yellow in fractures of olivine.
- Kelyphite – replacing garnet. Forms as fibrous/bladed crystals in a patchy texture. Mostly cryptocrystalline, but there are some visible grains of a light brown isotropic mineral that is most likely spinel, as well as larger fragments of possibly olivine or orthopyroxene (these show undulose extinction and low birefringence colours). There are also possibly some very small grains of talc (high birefringence – up to second order blue).

Sample: **89497**

Thin Section: 89497

Rock Name: Spinel Garnet Harzburgite

Texture: Coarse

Primary Mineralogy:

- 83% Olivine – Grains occur as anhedral crystals ranging in size from 10.8x7.1 mm to 0.8x0.32 mm. The larger grains show sub grains, and a couple have undulose extinction. Interference colours are up to second order blue, and a faint pink and green pleochroism is present.
- 10% Orthopyroxene – Grains occur as anhedral, highly fractured crystals with ragged edges. Sizes range from 3x2.6 mm to 0.2x0.2 mm, and some grains show a very faint pink pleochroism. Grains are present in both basal sections with two cleavages at 90 degrees, and longitudinal sections with one cleavage. Some grains show sub-grain boundaries.
- 5% Garnet – Grains occur as subhedral to anhedral crystals with kelyphitic rims. Sizes range from 2.6x2.7 mm to 1.2x0.72 mm. The majority of grains have been completely re-crystallized to kelyphite.
- 2% Spinel – Occurs as anhedral, mostly elongate, interstitial crystals ranging in size up to 0.76x0.24 mm.
- 1% Clinopyroxene – Grains are anhedral, ranging in size from 1.52x0.56 mm to 0.64x1.12 mm. A faint cleavage is present showing angular extinct. Grains also show a light green pleochroism and form in conjunction with orthopyroxene grains. Within one grain there is present a solid solution boundary between the two pyroxenes.
- 0.1% Biotite (?) – One grain visible with orangey-brown pleochroism and interference colours up to second order green. Grain is 0.28x0.24 mm in size. Also has parallel birds eye (?) extinction – Muscovite (?)

Secondary Minerals:

- Kelyphite – cryptocrystalline, with multiple layers each with a gradational change in crystal size coarsening outwards from garnet. Adjacent to garnet grain boundary is very fine layer of brown mineral, too fine to see individual grains thus looks like solid brown rim.

- Talc, or phlogopite (?), anhedral alteration in fractures of olivine and interstices, interference colours up to second order green and yellow.
- Calcite alteration in interstices.

Sample: **89487**

Thin Section: 89487

Rock Name: Spinel Harzburgite

Texture: Coarse

#### Primary Minerals:

- 82% Olivine – Grains occur as large anhedral highly fractured crystals ranging in size from 11.5x5.2 mm to 0.24x0.16 mm. Most grains have sub-grains and show undulose extinction. Tiny inclusions found along fractures in some grains.
- 12% Orthopyroxene – Grains occur as anhedral, highly fractured crystals ranging in size from 1.8x2 mm to 0.32x0.48 mm. Some longitudinal sections present showing one cleavage, most grains do not show any cleavage. Some grains have tiny inclusions following fracture patterns. Few grains have deformation twinning.
- 3% Spinel – Grains occur as anhedral elongate crystals ranging in size up to 0.8x0.24 mm. Grains seem to be overprinting pyroxene grains.
- 3% Clinopyroxene – Anhedral grains, 0.32x0.24 mm in size, showing light green pleochroism and lower relief than olivine. Interference colours are up to second order pink. Grains occur adjacent to, or surrounding, spinel grains.

#### Secondary Minerals:

- Serpentine alteration in fractures of olivine and interstices.
- Talc (or phlogopite (??)) in fractures of olivine and orthopyroxene, and in interstices.
- Calcite vein cuts through grains and across sample. Source is possibly from kimberlite (?) found at one end of thin section.



Sample: **89481**

Thins Section: 89481

Rock Name: Garnet clinopyroxenite

Texture: too altered to see a texture

Primary Minerals:

- 20% Garnet – Grains occur as subhedral to euhedral equant crystals with kelyphitic rims. Size ranges from >4.2x3.8 mm to 2.3x2.5 mm. Inclusions of clinopyroxene and talc (?) are present.
- 10% Clinopyroxene – Grains occur as euhedral to subhedral, tabular and equant crystals. Only longitudinal sections are present with one cleavage. Grain size ranges up to 1.8x0.56mm, and grains show sub-grains and undulose extinction.
- 1% Orthopyroxene – Grains occur as fractured, anhedral crystals showing low interference colours and parallel to sub-parallel extinction. Longitudinal sections are present with one cleavage. Size is 0.24x0.32 mm.
- 0.5% Olivine (?) – Grains occur as highly fractured, anhedral, equant crystals ranging in size from 0.76x1 mm to 0.32x0.4 mm, and showing higher relief than clinopyroxene.

Secondary Minerals:

- 70% Cryptocrystalline, yellowy-brown alteration entirely replacing clinopyroxene and groundmass minerals, likely serpentine and chlorite. There is also a dark rusty brown coloured mineral throughout the groundmass alteration, likely spinel.
- Kelyphite – brown, cryptocrystalline, with a radiating fibrous texture although texture is not as distinct as in previous samples.
- Calcite veining and alteration throughout sample.
- Talc around garnets and in fractures.

## **B. KIMBERLITE:**

Sample: **89496**

Thin Section: 89496A and B

Name: Phlogopite kimberlite

Texture: Macrocrystal

Primary Minerals:

15% Macrocrysts (>0.5 mm):

13% Olivine - Grains occur as subhedral, rounded, equant to elongate crystals ranging in size from 1.9x5 mm to 0.32x0.16 mm. Grains are quite fractured and some show undulose extinction. Birefringence colours are present up to second order yellow. Dynamic recrystallization has occurred in some grains.

1% Spinel – subhedral to euhedral grain, 0.24x0.32 mm in size.

1% Opaque mineral - subhedral to euhedral grain, 0.88x0.48 mm in size. Likely spinel.

85% Groundmass:

20% Microphenocrysts of olivine – grains occur as subhedral to euhedral, equant to elongate crystals ranging in size from 0.5 mm to 0.02 mm. Birefringence colours up to second order yellow are present. Some grains have been almost completely altered to serpentine, leaving a euhedral halo around a remnant grain. This is possibly monticellite (?).

15% Phlogopite – grains occur as euhedral, elongate crystals showing parallel extinction and birefringence colours up to first order grey. Grains range in size from 0.6x0.08 mm to 0.1x0.05 mm.

15% Serpentine – occurs as a fine grained aggregate between macrocrysts and microphenocrysts of olivine, showing grey/yellow birefringence colours.

15% Calcite – occurs as a fine grained aggregate between macrocrysts and microphenocrysts of olivine, showing high pastel birefringence colours.

- 13% Spinel – grains occur as subhedral to euhedral crystals ranging in size up to 0.8x0.4 mm. A dark reddy-brown colour and isotropism can be seen in the larger grains, but the smaller ones are opaque. These small opaque grains are identifiable as bead spinel from their nucleation on microphenocrysts. Atoll spinel is also present, making up approximately half of the spinel percentage. These grains are euhedral to subhedral cubic crystals, showing light brown colour in plain polar light and isotropism. Grains are surrounded by opaque rims/halos. Sizes range from 0.4x0.12 mm to 0.24x0.28 mm. There are also some anhedral grains present as inclusions in olivine macrocrysts.
- 5% Opaques – grains occur as subhedral to euhedral, equant crystals, ranging in size up to 0.28x0.2 mm. Most likely spinel.
- ~2% Perovskite - euhedral, equant, blackish-brown grains, showing high second order birefringence that is muted by dark colour. Grains range in size up to 40 µm in diameter.

#### Secondary Minerals:

- Serpentine replacing approximately 80% of the olivine macrocrysts on the outer margins. Some microphenocrysts also have replacement by serpentine.
- Calcite veins are present in two forms. The larger vein is 1.44 mm wide, and consists of medium grained equant crystals. The calcite overprints and surrounds the kimberlite material. The smaller vein crosscuts grains and is composed of elongate crystals.

Sample: **89495**

Thin Section: 89495A and B

Name: Carbonate, serpentine kimberlite

Texture: Macrocrystal

#### Primary Minerals:

15% Macrocrysts:

- 14% Olivine – grains occur as subhedral, rounded, equant to elongate crystals. Sizes range from 3.2x2.4 mm to 0.5 mm. Grains are highly fractured and altered to serpentine and carbonate. Some show undulose extinction.
- 1% Spinel – subhedral to euhedral, dark red, isotropic grains. Sizes range from 0.56x0.32 mm in size to 1.12x0.88 mm. The larger grain has a small olivine inclusion. Grains have opaque rims/halos, like atoll spinel.
- 85% Groundmass:
- 25% Serpentine – occurs as interstitial anhedral fibrous crystals showing pale yellow/white colour and grey birefringence.
- 15% Calcite – occurs as anhedral, fibrous crystals with ragged edges. Grains show low relief and high pastel birefringence.
- 18% Microphenocrysts of olivine – grains occur as subhedral to euhedral equant and elongate crystals ranging in size up to 0.5 mm. Grains are altered to serpentine, carbonate and phlogopite (?).
- 10% Phlogopite – subhedral to euhedral laths about 30x5 µm in size.
- 10% Spinel – occurs as bead spinel (small subhedral grains which nucleate around olivine microphenocrysts) and atoll spinel (euhedral cubic grains with halos and smaller opaque and non-opaque crystals between the core and halo). There is also a larger anhedral grain approximately 0.56x0.32 mm in size.
- 5% Opaque minerals – occurs as subhedral grains, ranging in size up to 0.06x0.06 mm.
- 1% Perovskite – occurs as subhedral to anhedral isotropic crystals, showing orangy-brown colour in plain polar light.
- ~1% Garnet – very small (0.24x0.16 mm) isotropic grains with opaque rims. Grains have high relief and are colourless in plain polar. One euhedral, equant inclusion approximately 0.36x0.22 mm in size is present inside an olivine macrocryst.

#### Secondary Minerals:

- Calcite replacing olivine forms as large euhedral crystals.
- Serpentine replacing olivine along fractures and around grain boundaries.
- Chlorite (?) replacing garnet.

Sample: **89486**

Thin Section: 89486A and B

Name: Phlogopite kimberlite

Texture: Macrocrystal

Primary Minerals:

- 10% Megacryst – irregular shaped grain 1.12x0.92 cm in size containing chlorite, carbonate, phlogopite laths, opaque minerals, possibly olivine, a dark brown epiclastic material, and a salmon coloured fibrous mineral that is possibly a mica.
- 15% Macrocrysts:
  - 14% Olivine – grains occur as subhedral, rounded, equant and elongate highly fractured crystals. Grains range in size from 2x2.1 mm to 0.5 mm. Some show undulose extinction and have serpentine, carbonate and phlogopite (?) alteration.
  - 1% Xenoliths – carbonate, highly altered to chlorite (?)
- 75% Groundmass:
  - 20% Microphenocrysts of olivine – occur as subhedral crystals with ragged edges ranging in size up to 0.5 mm.
  - 15% Calcite– occurs as anhedral patchy crystals with birefringence colours up to third order.
  - 15% Serpentine – occurs as anhedral patchy crystals with first order grey birefringence.
  - 15% Spinel - occurs as bead spinel (small subhedral grains which nucleate around olivine microphenocrysts) and atoll spinel (euhedral cubic crystals with halos). Most grains show some brown colour and isotropism. Grains range in size up to 0.28x0.24 mm.
  - 5% Opaque minerals – subhedral to anhedral equant grains ranging in size up to 0.15 mm. These are possibly the finer grain fraction of spinel and perovskite.
  - 0.5% Perovskite - euhedral, light brown, isotropic cubic grains with opaque rims. Grains are around 0.16 mm in size

Secondary Minerals:

- Serpentine replacing olivine macrocrysts.
- Calcite replacing olivine macrocrysts.

Sample: **89488**

Thin Section: 89488

Classification: Volcaniclastic kimberlite.

The sample is composed of two parts that will be described separately below. Classification of this sample as a whole is very difficult. The two materials described below are hard to distinguish between as there is only one area where a clear contact exists. At this contact there is a distinct difference in colour, sorting, and abundance of phenocrysts. A high concentration of small microphenocrysts of olivine (?) exists along the contact in the matrix of the darker material. Larger olivine microphenocrysts, present along the contact and slightly into the darker material, are surrounded by selvages of the lighter matrix. Throughout the rest of the sample the two materials have diffuse margins making them look intermixed, like two immiscible fluids.

Description One:

Rock Name: Volcaniclastic Kimberlite

The sample is composed of the following:

- 55% Discrete Macrocrysts - Olivine macrocrysts and microphenocrysts completely replaced by serpentine and carbonate. Grains are anhedral, mostly elongate, with some equant shapes. Sizes range up to 2.2 mm. Both the macrocrysts and microphenocrysts show rounded grain boundaries and a few of the larger macrocrysts have been fractured (or broken).
- 35% Light brown matrix, composed of:
- 57% Carbonate – very fine grained, almost cryptocrystalline.

- 35% Serpentine (?) – very fine grained, almost cryptocrystalline, showing low grey/blue birefringence.
- 3% Sedimentary (?) material – dark brown, non isotropic patches (possibly clasts) scattered throughout matrix. Some have small opaque grains within, and/or carbonate grains in and around them. Material looks similar to darker matrix described below.
- 2% Opaque minerals are subhedral to anhedral, and sometimes equant.
- 2% Spinel – Grains are subhedral, showing a dark brown colour and isotropism.
- 1% Phlogopite (?) laths are euhedral and range in size up to 40x230  $\mu\text{m}$ . Grains show birefringence colours up to second order yellow.
- 12% Lapilli (?) – Irregular shaped, with a higher concentration of phenocrysts, in a dark brown matrix. None are vesicular. Some are olivine cored, and most have very thin selvages. There are a couple cored by orthopyroxene grains, 100x30  $\mu\text{m}$  and 50x35  $\mu\text{m}$  in size. One large, sub-rounded, elongate xenolith, approximately 7.6x2.2 mm in size, is also present with a thin selvage surrounding it. The xenolith is composed of fine grained carbonate, with a coarse grained carbonate vein. Some olivine microphenocrysts have atoll spinel clustered around them.

#### Secondary Minerals:

- Carbonate replacing olivine forms as large anhedral crystals showing a mosaic texture usually in the centers of the grains.
- Serpentine is present replacing olivine. Grains are colourless and show blue birefringence.
- Opaque minerals are euhedral to anhedral, and occurring in four different forms. Large anhedral patches are present, as well as euhedral crystals, and euhedral needle-like grains. There are also small burr-like grains, possibly consisting of small opaque crystals with microfractures extending radially from them. All forms are present overprinting the serpentine/carbonate after olivine grains.

Comments:

Whether the fine grained material in the matrix mentioned above is actually of sedimentary composition or represents clasts of the other matrix material, cannot be determined by basic petrographic analysis. The designation of lapilli to the irregular shaped clasts of the darker matrix is tentative, as these “clasts” could merely be part of the patchy mixing distribution of the two different matrices.

Description Two:

Rock Name: Volcaniclastic kimberlite

The sample is composed of the following:

- 55% Discrete Macrocrysts - Olivine macrocrysts and microphenocrysts completely replaced by serpentine and carbonate. Grains are anhedral, rounded, mostly elongate, with some equant. Sizes range up to 2 mm. The macrocrysts and larger microphenocrysts show rounded grain boundaries and a few of the larger macrocrysts have been fractured (or broken). The smaller microphenocrysts show angular shapes; wedges are most common.
- 20% Lapilli - The majority of olivine grains have selvages of varying thickness and shape around them (composed of the lighter matrix material) forming juvenile lapilli. These juvenile lapilli form in erratic shapes pertaining to the olivine grains within them. Few are olivine cored.
- 25% Matrix - Dark brown matrix
  - 35% Carbonate - cryptocrystalline, with high pastel birefringence.
  - 35% Serpentine (?) – cryptocrystalline, yellow colour with low grey birefringence.
  - 10% Spinel (?) – dark, fine grained, cryptocrystalline
  - 20% Opaque minerals or ash - euhedral grains of about 5  $\mu\text{m}$  in size.
  - 3% Phlogopite (?) laths are euhedral and range in size up to 40x230  $\mu\text{m}$ .



#### Secondary Minerals:

- Carbonate replacing olivine forms as large anhedral crystals showing a mosaic texture usually in the centers of the grains. There is also carbonate occurring as crystals with a fibrous colloform texture around the grain edges of some olivines.
- Serpentine is present replacing olivine. Grains are yellow or colourless, and show yellow/blue birefringence.
- Chlorite (?) – subhedral, 35x15 µm in size, slight green pleochroism and anomalous blue birefringence.
- Opaque minerals are euhedral to anhedral, and occurring in four different forms. Large anhedral patches are present, as well as euhedral crystals, and euhedral needle-like grains. There are also small burr-like grains, possibly consisting of small opaque crystals with microfractures extending radially from them. All forms are present overprinting the serpentine/carbonate replaced olivine grains.
- Pectolite (?) / Apatite (?) – bright, reddy-orange, euhedral (?) aggregates of grains overprinting replaced olivine macrocrysts. Individual grains are microns in size and resemble fish roe.

#### Comments:

The source of the dark colour of the matrix is unknown. Possible sources include a high concentration of cryptocrystalline spinel, the presence of mud making the material epiclastic, or high concentrations of ash. The thin section is too thick for successful focusing of the matrix grains, and thus identification of the materials is limited to the outer edges of the sample.

#### Discussion:

The sample is thought to be volcanoclastic due to the restricted size distribution of olivine microphenocrysts and macrocrysts when compared to the more even distribution seen in the hypabyssal kimberlite samples. In the sample, smaller olivines have very uniform 160 µm and appear sorted. Other evidence for a volcanoclastic origin is the angular shapes of the olivines, the presence of lapilli, and the unusually dark and cryptocrystalline nature of the matrices. The irregular shapes and greater selvage thicknesses of the lapilli classify them as

juvenile lapilli, which are present in volcanoclastic non-tuffisitic kimberlite. A faint sorting and the possibility of the darker matrix consisting of sedimentary material point to a re-sedimented volcanoclastic (epiclastic) kimberlite classification. Although, the dark nature of the matrix could also be due to the presence of ash, or cryptocrystalline spinel, as has been mentioned above. Since none of these hypotheses can be proved by petrographic analysis, and further analytical techniques are beyond the scope of this description, the sample will be classified as a volcanoclastic kimberlite.

## Appendix II

### Electron Microprobe Analysis of Mantle Xenolith Samples

**Table 1 Composition of minerals in sample 89490B Xenolith B**

Mineral	Olivine											
Label	90B-13	90B-14	90B-15	90B-16	90B-17	90B-18	90B-19	90B-20	90B-21	90B-22	90B-23	Avg
Circle	9	9	10	10	10	10	10	11	11	11	11	
SiO <sub>2</sub>	40.66	40.86	40.32	40.96	40.08	40.96	40.44	41.31	40.77	41.03	40.58	40.72
TiO <sub>2</sub>	--	--	--	--	--	--	--	--	--	--	--	--
Al <sub>2</sub> O <sub>3</sub>	--	--	--	--	--	--	--	--	--	--	--	--
Cr <sub>2</sub> O <sub>3</sub>	--	--	--	--	--	--	--	--	--	--	--	--
FeO	8.07	8.00	7.83	8.03	8.04	7.93	8.29	8.05	8.02	8.11	8.03	8.04
MnO	0.12	0.15	0.17	0.13	0.08	0.09	0.10	0.14	0.13	0.11	0.11	0.12
MgO	50.55	50.53	50.50	50.56	50.76	50.48	50.24	50.56	50.58	50.63	50.41	50.53
CaO	0.05	0.09	0.08	0.06	0.05	0.10	0.08	0.08	0.09	0.08	0.05	0.07
Na <sub>2</sub> O	--	--	--	--	--	--	--	--	--	--	--	--
K <sub>2</sub> O	n/a	n/a	n/a	n/a	n/a	n/a	n/a	n/a	n/a	n/a	n/a	n/a
NiO	0.37	0.39	0.42	0.40	0.32	0.38	0.45	0.37	0.37	0.34	0.37	0.38
Total	99.91	100.15	99.34	100.20	99.49	100.08	99.73	100.67	100.06	100.48	99.70	99.98
Oxygens	4	4	4	4	4	4	4	4	4	4	4	4
Si <sup>4+</sup>	1.000	1.000	1.000	1.000	1.000	1.000	1.000	1.000	1.000	1.000	1.000	1.000
Ti <sup>4+</sup>	--	--	--	--	--	--	--	--	--	--	--	--
Al <sup>3+</sup>	--	--	--	--	--	--	--	--	--	--	--	--
Cr <sup>3+</sup>	--	--	--	--	--	--	--	--	--	--	--	--
Fe <sup>2+</sup>	0.166	0.164	0.162	0.164	0.168	0.162	0.172	0.163	0.165	0.165	0.166	0.165
Mn <sup>2+</sup>	0.003	0.003	0.004	0.003	0.002	0.002	0.002	0.003	0.003	0.002	0.002	0.003
Mg <sup>2+</sup>	1.853	1.843	1.867	1.840	1.887	1.837	1.852	1.825	1.849	1.839	1.852	1.849
Ca <sup>2+</sup>	0.001	0.002	0.002	0.002	0.001	0.003	0.002	0.002	0.002	0.002	0.001	0.002
Na <sup>+</sup>	--	--	--	--	--	--	--	--	--	--	--	--
K <sup>+</sup>	n/a	n/a	n/a	n/a	n/a	n/a	n/a	n/a	n/a	n/a	n/a	n/a
Ni <sup>2+</sup>	0.007	0.008	0.008	0.008	0.006	0.007	0.009	0.007	0.007	0.007	0.007	0.008
Total	3.032	3.024	3.044	3.017	3.068	3.014	3.040	3.005	3.029	3.021	3.032	3.030
Mg#	0.92	0.92	0.92	0.92	0.92	0.92	0.92	0.92	0.92	0.92	0.92	0.92

Here and Further:

-- = below MDL

n/a = not analysed

Table 2 Composition of minerals in sample 89490A and 89490B xenolith A

Mineral		Olivine															
Label	90A-3	90A-4	90A-5	90A-6	90A-7	90A-8	90A-9	90A-10	90A-11	90B-1	90B-4	90B-8	90B-9	90B-11	Avg		
Circle	7	7	7	7	7	8	8	8	8	3	3	6	6	7			
SiO <sub>2</sub>	40.96	40.18	40.69	39.64	40.73	40.37	40.84	40.19	41.26	40.29	40.63	40.93	40.63	40.42	40.55		
TiO <sub>2</sub>	--	--	--	--	--	--	--	--	--	--	--	--	--	--	--		
Al <sub>2</sub> O <sub>3</sub>	--	--	--	--	--	--	--	--	--	--	--	--	--	--	--		
Cr <sub>2</sub> O <sub>3</sub>	--	--	--	--	--	--	--	--	--	--	--	--	--	--	--		
FeO	8.98	8.78	8.87	8.99	8.88	9.10	8.89	8.94	9.03	8.97	9.12	8.96	9.09	8.93	8.97		
MnO	0.14	0.14	0.11	0.11	0.12	0.08	0.12	0.06	0.11	0.11	0.16	0.11	0.10	0.09	0.11		
MgO	49.71	49.83	49.70	49.92	49.59	49.62	49.69	49.50	49.64	49.69	49.60	49.95	49.97	49.61	49.72		
CaO	0.06	0.06	0.09	0.08	0.05	0.07	0.07	0.08	0.06	0.04	0.07	0.07	0.09	0.07	0.07		
Na <sub>2</sub> O	--	--	--	--	--	--	--	--	--	--	--	--	--	--	--		
K <sub>2</sub> O	n/a	n/a	n/a	n/a	n/a	n/a	n/a	n/a	n/a	n/a	n/a	n/a	n/a	n/a	n/a		
NiO	0.41	0.36	0.38	0.41	0.33	0.38	0.33	0.33	0.38	0.39	0.45	0.36	0.33	0.33	0.37		
Total	100.34	99.42	99.94	99.18	99.83	99.71	100.04	99.15	100.55	99.55	100.11	100.45	100.32	99.50	99.86		
Oxygens	4	4	4	4	4	4	4	4	4	4	4	4	4	4	4		
Si <sup>4+</sup>	1.000	1.000	1.000	1.000	1.000	1.000	1.000	1.000	1.000	1.000	1.000	1.000	1.000	1.000	1.000		
Ti <sup>4+</sup>	--	--	--	--	--	--	--	--	--	--	--	--	--	--	--		
Al <sup>3+</sup>	--	--	--	--	--	--	--	--	--	--	--	--	--	--	--		
Cr <sup>3+</sup>	--	--	--	--	--	--	--	--	--	--	--	--	--	--	--		
Fe <sup>2+</sup>	0.183	0.183	0.182	0.190	0.182	0.189	0.182	0.186	0.183	0.186	0.188	0.183	0.187	0.185	0.185		
Mn <sup>2+</sup>	0.003	0.003	0.002	0.002	0.003	0.002	0.002	0.001	0.002	0.002	0.003	0.002	0.002	0.002	0.002		
Mg <sup>2+</sup>	1.809	1.848	1.820	1.877	1.815	1.832	1.814	1.836	1.793	1.838	1.819	1.819	1.833	1.829	1.827		
Ca <sup>2+</sup>	0.001	0.002	0.002	0.002	0.001	0.002	0.002	0.002	0.001	0.001	0.002	0.002	0.002	0.002	0.002		
Na <sup>+</sup>	--	--	--	--	--	--	--	--	--	--	--	--	--	--	--		
K <sup>+</sup>	n/a	n/a	n/a	n/a	n/a	n/a	n/a	n/a	n/a	n/a	n/a	n/a	n/a	n/a	n/a		
Ni <sup>2+</sup>	0.008	0.007	0.007	0.008	0.007	0.008	0.006	0.007	0.007	0.008	0.009	0.007	0.007	0.007	0.007		
Total	3.007	3.045	3.018	3.080	3.011	3.035	3.009	3.034	2.989	3.038	3.023	3.015	3.035	3.026	3.026		
Mg#	0.91	0.91	0.91	0.91	0.91	0.91	0.91	0.91	0.91	0.91	0.91	0.91	0.91	0.91	0.91		

Table 2 continued

Mineral				Clinopyroxene												Garnet			
Label	90B-2	90B-8	90A-13	Avg	90B-12	90A-1	90A-2	90A-3	90A-4	90A-5	90A-6	90A-8	90A-10	90A-9	90B-1	90B-2	Avg		
Circle	1	1	4	5	8	1	1	1	2	2	4	5	6	5	1	1			
SiO <sub>2</sub>	57.35	57.31	57.24	57.30	54.32	41.97	41.79	41.63	41.86	41.69	41.75	41.68	41.76	41.37	41.76	41.72	41.73		
TiO <sub>2</sub>	0.11	0.13	0.11	0.12	0.16	0.47	0.42	0.43	0.48	0.50	0.47	0.49	0.44	0.46	0.46	0.45	0.46		
Al <sub>2</sub> O <sub>3</sub>	0.77	0.73	0.76	0.75	0.65	21.01	21.14	21.03	21.03	20.99	20.89	20.90	20.92	20.87	21.03	20.98	20.98		
Cr <sub>2</sub> O <sub>3</sub>	0.26	0.26	0.22	0.24	0.96	3.11	3.08	3.02	3.08	3.01	3.10	3.14	3.05	3.03	3.00	3.15	3.07		
FeO	5.52	5.64	5.62	5.59	2.94	7.47	7.53	7.76	7.57	7.73	7.69	7.68	7.76	7.82	7.98	7.58	7.69		
MnO	0.14	0.15	0.13	0.14	0.11	0.25	0.31	0.26	0.29	0.33	0.32	0.28	0.35	0.27	0.33	0.34	0.30		
MgO	33.82	34.03	33.99	33.95	18.90	20.84	20.77	20.82	20.62	20.82	20.75	20.66	20.77	20.64	20.87	20.96	20.77		
CaO	0.89	0.88	0.87	0.88	19.99	4.62	4.56	4.60	4.52	4.58	4.47	4.55	4.53	4.54	4.53	4.56	4.55		
Na <sub>2</sub> O	0.16	0.19	0.15	0.17	0.79	--	--	--	--	--	--	--	--	--	--	--	--		
K <sub>2</sub> O	--	--	--	--	--	n/a	n/a	n/a	n/a	n/a	n/a	n/a	n/a	n/a	n/a	n/a	n/a		
NiO	n/a	n/a	n/a	n/a	n/a	n/a	n/a	n/a	n/a	n/a	n/a	n/a	n/a	n/a	n/a	n/a	n/a		
Total	99.02	99.33	99.10	99.15	98.82	99.80	99.65	99.59	99.48	99.69	99.49	99.43	99.62	99.04	100.04	99.79	99.60		
Oxygens	6	6	6	6	6	7	7	7	7	7	7	7	7	7	7	7	7		
Si <sup>4+</sup>	1.992	1.986	1.987	1.988	1.986	2.998	2.990	2.984	3.000	2.986	2.995	2.992	2.994	2.984	2.984	2.985	2.990		
Ti <sup>4+</sup>	0.003	0.003	0.003	0.003	0.004	0.026	0.023	0.023	0.026	0.027	0.025	0.027	0.024	0.025	0.025	0.024	0.025		
Al <sup>3+</sup>	0.032	0.030	0.031	0.031	0.028	1.769	1.783	1.777	1.776	1.772	1.766	1.768	1.767	1.774	1.771	1.769	1.772		
Cr <sup>3+</sup>	0.007	0.007	0.006	0.007	0.028	0.176	0.174	0.171	0.174	0.170	0.176	0.178	0.173	0.173	0.170	0.178	0.174		
Fe <sup>2+</sup>	0.160	0.164	0.163	0.162	0.090	0.447	0.451	0.465	0.453	0.463	0.461	0.461	0.465	0.472	0.477	0.454	0.461		
Mn <sup>2+</sup>	0.004	0.004	0.004	0.004	0.003	0.015	0.019	0.016	0.017	0.020	0.020	0.017	0.021	0.017	0.020	0.021	0.018		
Mg <sup>2+</sup>	1.751	1.758	1.759	1.756	1.030	2.219	2.215	2.225	2.203	2.223	2.218	2.210	2.219	2.219	2.223	2.235	2.219		
Ca <sup>2+</sup>	0.033	0.033	0.032	0.033	0.783	0.354	0.350	0.353	0.347	0.352	0.344	0.350	0.348	0.351	0.347	0.349	0.349		
Na <sup>+</sup>	0.011	0.013	0.010	0.011	0.056	--	--	--	--	--	--	--	--	--	--	--	--		
K <sup>+</sup>	--	--	--	--	--	n/a	n/a	n/a	n/a	n/a	n/a	n/a	n/a	n/a	n/a	n/a	n/a		
Ni <sup>2+</sup>	n/a	n/a	n/a	n/a	n/a	n/a	n/a	n/a	n/a	n/a	n/a	n/a	n/a	n/a	n/a	n/a	n/a		
Total	3.992	3.999	3.996	3.996	4.010	8.008	8.012	8.022	8.003	8.019	8.013	8.011	8.017	8.021	8.025	8.022	8.016		
Mg#	0.92	0.91	0.92	0.92	0.92	0.83	0.83	0.83	0.83	0.83	0.83	0.83	0.83	0.82	0.82	0.83	0.83		

[illegible]

Table 3 continued

Mineral		Orthopyroxene																			
Label		94-1	94-4	94-2	494-1	494-2	494-3	494-4	494-5	494-15	494-16	494-18	494-19	494-20	494-22	494-23	494-25	494-28	494-29	Avg	
Circle		1	1	1	3	3	3	4	4	2	2	1	1	1	6	6	6	7	7		
SiO <sub>2</sub>		57.11	57.34	57.82	56.70	57.27	56.90	57.26	56.59	56.87	57.09	56.85	56.69	56.81	56.81	56.64	56.81	57.02	56.52	56.95	
TiO <sub>2</sub>		0.23	0.22	0.22	0.23	0.22	0.25	0.19	0.20	0.20	0.21	0.22	0.24	0.24	0.18	0.20	0.20	0.21	0.23	0.22	
Al <sub>2</sub> O <sub>3</sub>		0.68	0.69	0.68	0.67	0.70	0.67	0.67	0.71	0.67	0.68	0.69	0.67	0.66	0.70	0.66	0.72	0.68	0.71	0.68	
Cr <sub>2</sub> O <sub>3</sub>		0.25	0.23	0.21	0.24	0.25	0.21	0.25	0.21	0.25	0.17	0.26	0.24	0.17	0.30	0.25	0.23	0.22	0.27	0.23	
FeO		5.27	5.38	5.23	5.32	5.30	5.65	5.42	5.62	5.37	5.42	5.37	5.24	5.37	5.43	5.46	5.25	5.31	5.35	5.37	
MnO		0.16	0.12	0.11	0.16	0.14	0.10	0.11	0.13	--	0.11	0.13	0.14	--	0.14	0.11	--	0.15	0.19	0.12	
MgO		34.71	34.77	34.56	34.72	34.52	34.59	34.77	34.52	34.69	34.65	34.70	34.80	34.66	34.69	34.70	34.70	34.61	34.69	34.67	
CaO		0.91	0.93	0.87	0.94	0.92	0.93	0.88	0.96	0.95	1.00	0.91	0.94	0.97	0.99	0.99	0.97	0.95	0.92	0.94	
Na <sub>2</sub> O		0.15	0.12	0.11	0.16	0.15	0.15	0.11	0.15	0.15	0.11	0.13	0.12	0.14	0.12	0.10	0.10	0.13	0.14	0.13	
K <sub>2</sub> O	--	--	--	--	--	--	--	--	--	--	--	--	--	--	--	--	--	--	--	--	
NiO	n/a	n/a	n/a	n/a	n/a	n/a	n/a	n/a	n/a	n/a	n/a	n/a	n/a	n/a	n/a	n/a	n/a	n/a	n/a	n/a	
Total		99.46	99.80	99.84	99.13	99.48	99.45	99.66	99.10	99.22	99.45	99.26	99.06	99.09	99.35	99.12	99.06	99.28	99.03	99.32	
Oxygens		6	6	6	6	6	6	6	6	6	6	6	6	6	6	6	6	6	6	6	
Si <sup>4+</sup>		1.976	1.989	1.977	1.970	1.980	1.972	1.977	1.969	1.973	1.976	1.972	1.970	1.973	1.970	1.969	1.973	1.976	1.967	1.974	
Ti <sup>4+</sup>		0.006	0.006	0.006	0.006	0.006	0.007	0.005	0.005	0.005	0.006	0.006	0.006	0.006	0.005	0.005	0.005	0.006	0.006	0.006	
Al <sup>3+</sup>		0.028	0.028	0.028	0.028	0.029	0.027	0.027	0.029	0.028	0.028	0.028	0.027	0.027	0.029	0.027	0.029	0.028	0.029	0.028	
Cr <sup>3+</sup>		0.007	0.006	0.006	0.007	0.007	0.006	0.007	0.006	0.007	0.005	0.007	0.007	0.005	0.008	0.007	0.006	0.006	0.007	0.006	
Fe <sup>2+</sup>		0.152	0.151	0.155	0.154	0.153	0.164	0.156	0.164	0.156	0.157	0.156	0.152	0.156	0.157	0.159	0.152	0.154	0.156	0.156	
Mn <sup>2+</sup>		0.005	0.003	0.003	0.005	0.004	0.003	0.003	0.004	--	0.003	0.004	0.004	--	0.004	0.003	0.002	--	0.006	0.004	
Mg <sup>2+</sup>		1.789	1.772	1.787	1.798	1.779	1.787	1.789	1.790	1.794	1.787	1.794	1.802	1.795	1.793	1.798	1.796	1.788	1.799	1.791	
Ca <sup>2+</sup>		0.034	0.032	0.034	0.035	0.034	0.035	0.033	0.036	0.035	0.037	0.034	0.035	0.036	0.037	0.037	0.036	0.035	0.034	0.035	
Na <sup>+</sup>		0.010	0.008	0.008	0.011	0.010	0.010	0.008	0.010	0.010	0.008	0.009	0.008	0.009	0.008	0.007	0.007	0.009	0.010	0.009	
K <sup>+</sup>	--	--	--	--	--	--	--	--	--	--	--	--	--	--	--	--	--	--	--	--	
Ni <sup>2+</sup>	n/a	n/a	n/a	n/a	n/a	n/a	n/a	n/a	n/a	n/a	n/a	n/a	n/a	n/a	n/a	n/a	n/a	n/a	n/a	n/a	
Total		4.006	3.993	4.005	4.013	4.002	4.010	4.005	4.013	4.010	4.006	4.009	4.011	4.009	4.011	4.012	4.008	4.006	4.014	4.008	
Mg#		0.92	0.92	0.92	0.92	0.92	0.92	0.92	0.92	0.92	0.92	0.92	0.92	0.92	0.92	0.92	0.92	0.92	0.92	0.92	

Table 3 continued

Mineral	Clinopyroxene				Garnet					
Label	494-8	494-10	494-14	Avg	94-1	94-3	94-4	94-5	94-2	Avg
Circle	5	5	3		1	1	1	1	1	
SiO <sub>2</sub>	54.34	54.56	54.08	54.33	42.05	41.91	41.84	41.99	41.47	41.85
TiO <sub>2</sub>	0.31	0.30	0.33	0.31	0.43	0.31	0.34	0.34	0.33	0.35
Al <sub>2</sub> O <sub>3</sub>	1.49	1.50	1.50	1.50	21.64	21.61	21.78	21.57	21.58	21.64
Cr <sub>2</sub> O <sub>3</sub>	0.84	0.78	0.79	0.80	2.68	2.75	2.70	2.59	2.76	2.70
FeO	3.25	3.14	3.09	3.16	7.23	7.13	7.16	7.18	7.40	7.22
MnO	0.13	0.12	0.12	0.12	0.27	0.26	0.32	0.31	0.28	0.29
MgO	18.96	18.85	19.02	18.94	21.14	20.99	21.19	21.03	21.21	21.11
CaO	18.59	18.68	18.86	18.71	4.43	4.53	4.53	4.39	4.54	4.48
Na <sub>2</sub> O	1.08	1.07	1.16	1.10	--	--	--	--	--	--
K <sub>2</sub> O	--	--	--	--	n/a	n/a	n/a	n/a	n/a	n/a
NiO	n/a	n/a	n/a	n/a	n/a	n/a	n/a	n/a	n/a	n/a
Total	99.06	99.06	99.02	99.04	99.93	99.53	99.90	99.45	99.61	99.68
Oxygens	6	6	6	6	7	7	7	7	7	7
Si <sup>4+</sup>	1.978	1.983	1.971	1.977	2.990	2.992	2.978	2.998	2.966	2.985
Ti <sup>4+</sup>	0.009	0.008	0.009	0.009	0.023	0.017	0.018	0.018	0.018	0.019
Al <sup>3+</sup>	0.064	0.065	0.065	0.064	1.814	1.818	1.826	1.816	1.819	1.818
Cr <sup>3+</sup>	0.024	0.022	0.023	0.023	0.151	0.155	0.152	0.146	0.156	0.152
Fe <sup>2+</sup>	0.099	0.095	0.094	0.096	0.430	0.425	0.426	0.429	0.443	0.431
Mn <sup>2+</sup>	0.004	0.004	0.004	0.004	0.016	0.016	0.020	0.019	0.017	0.017
Mg <sup>2+</sup>	1.028	1.021	1.033	1.028	2.241	2.233	2.248	2.238	2.261	2.244
Ca <sup>2+</sup>	0.725	0.728	0.736	0.730	0.337	0.346	0.345	0.336	0.348	0.342
Na <sup>+</sup>	0.077	0.075	0.082	0.078	--	--	--	--	--	--
K <sup>+</sup>	--	--	--	--	n/a	n/a	n/a	n/a	n/a	n/a
Ni <sup>2+</sup>	n/a	n/a	n/a	n/a	n/a	n/a	n/a	n/a	n/a	n/a
Total	4.010	4.004	4.020	4.011	8.008	8.007	8.017	8.005	8.032	8.014
Mg#	0.91	0.91	0.92	0.91	0.84	0.84	0.84	0.84	0.84	0.84



Table 4 Composition of minerals in sample 89481

Mineral Label	Orthopyroxene					Clinopyroxene					Garnet						
	81-5	81-6	81-10	81-11	Avg	81-8	81-1	81-2	81-3	81-4	81-5	81-6	81-7	81-8	81-9	81-10	Avg
Circle	3	3	5	5		4	1	1	2	2	3	3	4	4	5	5	
SiO <sub>2</sub>	57.25	57.28	57.39	57.26	57.30	54.87	41.93	41.87	41.68	42.03	41.95	41.64	41.64	42.05	41.57	41.53	41.79
TiO <sub>2</sub>	0.12	0.16	0.10	0.12	0.13	0.14	0.36	0.38	0.36	0.36	0.35	0.36	0.37	0.37	0.42	0.38	0.37
Al <sub>2</sub> O <sub>3</sub>	0.58	0.57	0.51	0.57	0.56	2.00	21.30	21.25	21.25	21.23	21.53	21.19	21.34	21.40	21.18	20.97	21.27
Cr <sub>2</sub> O <sub>3</sub>	0.24	--	0.23	0.21	0.21	1.36	3.34	3.35	3.47	3.35	3.43	3.42	3.44	3.39	3.43	3.36	3.40
FeO	5.18	5.12	5.22	5.17	5.17	2.69	7.57	7.37	7.34	7.28	7.45	7.30	7.23	7.32	7.35	7.37	7.36
MnO	0.12	0.10	0.12	0.14	0.12	0.11	0.29	0.25	0.34	0.34	0.30	0.34	0.33	0.37	0.34	0.34	0.32
MgO	35.17	35.35	35.20	35.06	35.19	17.38	20.91	20.62	20.83	20.72	20.80	20.84	20.80	20.81	20.56	20.50	20.74
CaO	0.62	0.67	0.56	0.61	0.61	19.01	4.53	4.55	4.57	4.62	4.57	4.61	4.55	4.59	4.47	4.55	4.56
Na <sub>2</sub> O	0.11	0.11	0.10	0.12	0.11	1.60	--	--	--	--	--	--	--	--	--	--	--
K <sub>2</sub> O	--	--	--	--	--	--	n/a	n/a	n/a	n/a	n/a	n/a	n/a	n/a	n/a	n/a	n/a
NiO	n/a	n/a	n/a	n/a	n/a	n/a	n/a	n/a	n/a	n/a	n/a	n/a	n/a	n/a	n/a	n/a	n/a
Total	99.38	99.53	99.46	99.26	99.41	99.21	100.29	99.68	99.89	100.00	100.43	99.76	99.74	100.35	99.37	99.06	99.86
Oxygens	6	6	6	6	6	6	7	7	7	7	7	7	7	7	7	7	7
Si <sup>4+</sup>	1.979	1.977	1.982	1.981	1.980	1.992	2.983	2.993	2.977	2.995	2.979	2.978	2.976	2.987	2.983	2.991	2.984
Ti <sup>4+</sup>	0.003	0.004	0.003	0.003	0.003	0.004	0.019	0.020	0.020	0.020	0.019	0.020	0.020	0.020	0.023	0.020	0.020
Al <sup>3+</sup>	0.024	0.023	0.021	0.023	0.023	0.086	1.786	1.791	1.789	1.783	1.802	1.786	1.798	1.792	1.792	1.780	1.790
Cr <sup>3+</sup>	0.006	--	0.006	0.006	0.006	0.039	0.188	0.189	0.196	0.189	0.193	0.193	0.194	0.191	0.195	0.191	0.192
Fe <sup>2+</sup>	0.150	0.148	0.151	0.150	0.149	0.082	0.450	0.440	0.438	0.434	0.442	0.437	0.432	0.435	0.441	0.444	0.439
Mn <sup>2+</sup>	0.004	0.003	0.004	0.004	0.004	0.003	0.018	0.015	0.020	0.020	0.018	0.021	0.020	0.023	0.021	0.021	0.020
Mg <sup>2+</sup>	1.812	1.818	1.812	1.808	1.812	0.940	2.218	2.197	2.218	2.201	2.201	2.222	2.217	2.203	2.199	2.201	2.208
Ca <sup>2+</sup>	0.023	0.025	0.021	0.022	0.023	0.739	0.345	0.348	0.350	0.353	0.348	0.353	0.348	0.349	0.344	0.351	0.349
Na <sup>+</sup>	0.008	0.007	0.007	0.008	0.007	0.112	--	--	--	--	--	--	--	--	--	--	--
K <sup>+</sup>	--	--	--	--	--	--	n/a	n/a	n/a	n/a	n/a	n/a	n/a	n/a	n/a	n/a	n/a
Ni <sup>2+</sup>	n/a	n/a	n/a	n/a	n/a	n/a	n/a	n/a	n/a	n/a	n/a	n/a	n/a	n/a	n/a	n/a	n/a
Total	4.007	4.009	4.006	4.005	4.007	3.999	8.015	8.001	8.014	8.003	8.009	8.017	8.010	8.006	8.004	8.007	8.008
Mg#	0.92	0.92	0.92	0.92	0.92	0.92	0.83	0.83	0.83	0.84	0.83	0.84	0.84	0.84	0.83	0.83	0.83

Table 5 Composition of minerals in sample 89497

Major components of minerals in sample 99-101																															
Mineral			Olivine										Clinopyroxene										Garnet								
Label	97-1	97-3	97-4	97-8	97-9	97-10	97-11	Avg			497-22	497-23	497-24	Avg			97-1	97-2	97-3	97-4	97-6	Avg			97-1	97-2	97-3	97-4	97-6	Avg	
Circle	1	3	3	8	8	9	9	9			1	1	1	1			4	4	5	6	10					4	4	5	6	10	
SiO <sub>2</sub>	41.34	41.51	40.86	40.86	41.52	40.84	41.32	41.18			53.84	54.35	54.13	54.11			40.53	41.10	41.01	40.64	40.92	40.84			40.53	41.10	41.01	40.64	40.92	40.84	
TiO <sub>2</sub>	--	--	--	--	--	--	--	--	--	--	--	--	--	--	--	--	--	--	--	--	--	--	--	--	--	--	--	--	--	--	--
Al <sub>2</sub> O <sub>3</sub>	--	--	--	--	--	--	--	--	--	--	0.99	1.00	0.96	0.99			18.87	18.90	19.14	18.69	18.85	18.89			18.87	18.90	19.14	18.69	18.85	18.89	
Cr <sub>2</sub> O <sub>3</sub>	--	--	--	--	--	--	--	--	--	--	0.90	0.82	0.81	0.85			7.21	6.89	7.22	7.64	7.25	7.24			7.21	6.89	7.22	7.64	7.25	7.24	
FeO	7.74	7.58	7.63	7.46	7.45	7.31	7.51	7.53			1.21	1.18	1.19	1.19			7.39	7.46	7.57	7.49	7.71	7.53			7.39	7.46	7.57	7.49	7.71	7.53	
MnO	0.10	0.10	0.10	0.14	0.11	0.09	0.10	0.10			0.12	--	--	--			0.48	0.48	0.46	0.51	0.50	0.49			0.48	0.48	0.46	0.51	0.50	0.49	
MgO	50.90	50.85	50.67	50.59	50.55	50.78	50.62	50.71			17.57	17.61	17.60	17.60			17.72	17.85	17.95	17.53	17.39	17.69			17.72	17.85	17.95	17.53	17.39	17.69	
CaO	--	--	0.04	--	0.05	0.04	0.06	0.04			23.81	23.46	23.76	23.68			7.07	6.97	7.03	7.27	7.30	7.13			7.07	6.97	7.03	7.27	7.30	7.13	
Na <sub>2</sub> O	--	--	--	--	--	--	--	--	--	--	0.67	0.64	0.63	0.65			--	--	--	--	--	--	--	--	--	--	--	--	--	--	--
K <sub>2</sub> O	n/a	n/a	n/a	n/a	n/a	n/a	n/a	n/a	n/a	n/a	--	--	--	--			n/a	n/a	n/a	n/a	n/a	n/a	n/a	n/a	n/a	n/a	n/a	n/a	n/a	n/a	n/a
NiO	0.26	0.32	0.41	0.34	0.40	0.34	0.34	0.34			n/a	n/a	n/a	n/a			n/a	n/a	n/a	n/a	n/a	n/a	n/a	n/a	n/a	n/a	n/a	n/a	n/a	n/a	n/a
Total	100.39	100.40	99.82	99.45	100.13	99.41	100.04	99.95			99.11	99.19	99.10	99.13			99.27	99.67	100.37	99.79	99.95	99.81			99.27	99.67	100.37	99.79	99.95	99.81	
Oxygens																															
Si <sup>4+</sup>	1.000	1.000	1.000	1.000	1.000	1.000	1.000	1.000			1.970	1.982	1.978	1.976			2.974	2.998	2.975	2.973	2.987	2.981			2.974	2.998	2.975	2.973	2.987	2.981	
Ti <sup>4+</sup>	--	--	--	--	--	--	--	--	--	--	--	--	--	--			--	--	--	--	--	--	--	--	--	--	--	--	--	--	--
Al <sup>3+</sup>	--	--	--	--	--	--	--	--	--	--	0.043	0.043	0.041	0.042			1.632	1.625	1.636	1.612	1.621	1.625			1.632	1.625	1.636	1.612	1.621	1.625	
Cr <sup>3+</sup>	--	--	--	--	--	--	--	--	--	--	0.026	0.024	0.024	0.024			0.418	0.398	0.414	0.442	0.419	0.418			0.418	0.398	0.414	0.442	0.419	0.418	
Fe <sup>2+</sup>	0.157	0.153	0.156	0.153	0.150	0.150	0.152	0.153			0.037	0.036	0.037	0.036			0.454	0.455	0.459	0.458	0.471	0.459			0.454	0.455	0.459	0.458	0.471	0.459	
Mn <sup>2+</sup>	0.002	0.002	0.002	0.003	0.002	0.002	0.002	0.002			0.004	--	--	--			0.030	0.030	0.028	0.032	0.031	0.030			0.030	0.030	0.028	0.032	0.031	0.030	
Mg <sup>2+</sup>	1.835	1.826	1.848	1.845	1.815	1.853	1.826	1.836			0.959	0.957	0.959	0.958			1.938	1.941	1.941	1.912	1.892	1.925			1.938	1.941	1.941	1.912	1.892	1.925	
Ca <sup>2+</sup>	--	--	0.001	--	0.001	0.001	0.002	0.001			0.934	0.917	0.930	0.927			0.556	0.545	0.546	0.570	0.571	0.558			0.556	0.545	0.546	0.570	0.571	0.558	
Na <sup>+</sup>	--	--	--	--	--	--	--	--	--	--	0.048	0.046	0.045	0.046			--	--	--	--	--	--	--	--	--	--	--	--	--	--	--
K <sup>+</sup>	n/a	n/a	n/a	n/a	n/a	n/a	n/a	n/a	n/a	n/a	--	--	--	--			n/a	n/a	n/a	n/a	n/a	n/a	n/a	n/a	n/a	n/a	n/a	n/a	n/a	n/a	n/a
Ni <sup>2+</sup>	0.005	0.006	0.008	0.007	0.008	0.007	0.007	0.007			n/a	n/a	n/a	n/a			n/a	n/a	n/a	n/a	n/a	n/a	n/a	n/a	n/a	n/a	n/a	n/a	n/a	n/a	n/a
Total	3.001	2.988	3.018	3.009	2.978	3.013	2.990	2.999			4.019	4.007	4.013	4.013			8.002	7.992	8.001	8.000	7.994	7.997			8.002	7.992	8.001	8.000	7.994	7.997	
Mg#	0.92	0.92	0.92	0.92	0.92	0.93	0.92	0.92			0.96	0.96	0.96	0.96			0.81	0.81	0.81	0.81	0.80	0.81			0.81	0.81	0.81	0.81	0.80	0.81	

Table 5 continued

Mineral		Orthopyroxene																			
Label	497-1	497-2	497-3	497-5	497-7	497-8	497-9	497-10	497-11	497-12	497-13	497-14	497-15	497-16	497-20	497-21	497-25	497-26	Avg		
Circle	7	7	7	8	6	6	4	4	4	3	3	5	5	5	2	2	1	1	1		
SiO <sub>2</sub>	57.22	56.97	57.31	57.40	57.58	57.06	57.43	56.94	57.53	56.82	57.37	57.37	57.21	57.21	57.05	57.71	57.26	57.53	57.28		
TiO <sub>2</sub>	--	--	--	--	--	--	--	--	--	--	--	--	--	--	--	--	--	--	--		
Al <sub>2</sub> O <sub>3</sub>	0.65	0.63	0.61	0.63	0.65	0.65	0.64	0.63	0.65	0.61	0.64	0.62	0.60	0.64	0.60	0.62	0.64	0.62	0.63		
Cr <sub>2</sub> O <sub>3</sub>	0.20	0.23	0.23	0.18	0.20	0.23	0.18	0.19	0.20	0.28	0.20	0.19	0.24	0.24	0.21	0.25	0.21	0.21	0.22		
FeO	4.48	4.69	4.65	4.69	4.44	4.72	4.60	4.65	4.69	4.62	4.64	4.78	4.74	4.63	4.62	4.52	4.77	4.51	4.63		
MnO	0.15	0.13	0.11	0.09	0.10	0.11	0.09	0.20	0.07	0.10	0.12	0.13	0.14	0.17	0.09	0.12	0.13	0.11	0.12		
MgO	36.19	36.26	36.47	36.30	36.25	36.05	36.20	36.21	36.18	36.22	36.30	36.24	36.13	36.10	36.20	36.37	36.14	36.36	36.23		
CaO	0.24	0.23	0.24	0.24	0.21	0.27	0.21	0.26	0.22	0.26	0.24	0.23	0.23	0.25	0.23	0.23	0.24	0.24	0.24		
Na <sub>2</sub> O	--	--	--	--	--	--	--	--	--	--	--	--	--	--	--	--	--	--	--		
K <sub>2</sub> O	--	--	--	--	--	--	--	--	--	--	--	--	--	--	--	--	--	--	--		
NiO	n/a	n/a	n/a	n/a	n/a	n/a	n/a	n/a	n/a	n/a	n/a	n/a	n/a	n/a	n/a	n/a	n/a	n/a	n/a		
Total	99.14	99.17	99.66	99.58	99.45	99.12	99.37	99.09	99.55	98.94	99.55	99.61	99.32	99.25	99.04	99.82	99.40	99.59	99.37		
Oxygens																					
Si <sup>4+</sup>	1.974	1.968	1.969	1.973	1.979	1.972	1.977	1.969	1.977	1.967	1.973	1.973	1.973	1.973	1.972	1.977	1.973	1.976	1.973		
Ti <sup>4+</sup>	--	--	--	--	--	--	--	--	--	--	--	--	--	--	--	--	--	--	--		
Al <sup>3+</sup>	0.026	0.026	0.025	0.025	0.026	0.027	0.026	0.026	0.026	0.025	0.026	0.025	0.024	0.026	0.025	0.025	0.026	0.025	0.026		
Cr <sup>3+</sup>	0.005	0.006	0.006	0.005	0.005	0.006	0.005	0.005	0.005	0.008	0.005	0.005	0.007	0.007	0.006	0.007	0.006	0.006	0.006		
Fe <sup>2+</sup>	0.129	0.136	0.134	0.135	0.128	0.136	0.133	0.134	0.135	0.134	0.134	0.137	0.137	0.134	0.133	0.129	0.137	0.130	0.134		
Mn <sup>2+</sup>	0.004	0.004	0.003	0.003	0.003	0.003	0.003	0.006	0.002	0.003	0.004	0.004	0.004	0.005	0.003	0.003	0.004	0.003	0.003		
Mg <sup>2+</sup>	1.861	1.867	1.868	1.860	1.856	1.857	1.857	1.866	1.853	1.869	1.861	1.857	1.857	1.856	1.865	1.857	1.856	1.861	1.860		
Ca <sup>2+</sup>	0.009	0.009	0.009	0.009	0.008	0.010	0.008	0.010	0.008	0.010	0.009	0.008	0.008	0.009	0.009	0.008	0.009	0.009	0.009		
Na <sup>+</sup>	--	--	--	--	--	--	--	--	--	--	--	--	--	--	--	--	--	--	--		
K <sup>+</sup>	--	--	--	--	--	--	--	--	--	--	--	--	--	--	--	--	--	--	--		
Ni <sup>2+</sup>	n/a	n/a	n/a	n/a	n/a	n/a	n/a	n/a	n/a	n/a	n/a	n/a	n/a	n/a	n/a	n/a	n/a	n/a	n/a		
Total	4.011	4.016	4.017	4.012	4.007	4.013	4.008	4.016	4.007	4.018	4.012	4.014	4.011	4.010	4.014	4.008	4.012	4.009	4.012		
Mg#	0.94	0.93	0.93	0.93	0.94	0.93	0.93	0.93	0.93	0.93	0.93	0.93	0.93	0.93	0.93	0.93	0.93	0.93	0.93		

Table 5 continued

Mineral		Spinel															
Label		97-9	97-2	97-4	Avg	97-8	97-3	97-5	97-7	97-18	Avg	97-14	97-13	97-11	97-12	Avg	97-10
Circle		3	1	1		3	1	2	2	9		8	8	7	7		7
SiO <sub>2</sub>		0.07	0.01	0.04	0.04	0.03	0.04	0.03	0.02	0.03	0.03	0.06	0.08	0.03	0.01	0.02	0.04
TiO <sub>2</sub>	--	--	0.05	0.05	--	0.10	0.05	0.05	--	--	--	0.07	1.05	--	--	--	0.64
Al <sub>2</sub> O <sub>3</sub>	14.25	14.41	14.40	14.40	14.35	13.51	14.53	14.70	14.67	14.30	14.56	14.14	11.68	13.64	13.77	13.70	12.55
Cr <sub>2</sub> O <sub>3</sub>	57.61	57.66	58.01	57.76	56.83	56.83	57.19	56.75	57.09	56.73	56.86	57.44	56.64	57.03	56.82	56.92	56.72
FeO	13.11	12.85	12.96	12.97	14.36	14.36	13.24	13.00	13.32	13.09	13.14	13.26	15.52	14.57	14.81	14.69	15.82
MnO	0.10	0.09	0.08	0.09	--	--	0.09	--	0.14	0.13	0.10	0.09	0.12	0.11	0.21	0.16	0.18
MgO	14.66	14.44	14.52	14.54	14.48	14.48	14.33	14.44	14.12	14.44	14.33	14.41	14.07	13.62	13.35	13.48	13.59
CaO	--	--	--	--	0.04	0.04	--	--	--	0.08	0.04	--	0.04	--	--	--	--
Na <sub>2</sub> O	n/a	n/a	n/a	n/a	n/a	n/a	n/a	n/a	n/a	n/a	n/a	n/a	n/a	n/a	n/a	n/a	n/a
K <sub>2</sub> O	n/a	n/a	n/a	n/a	n/a	n/a	n/a	n/a	n/a	n/a	n/a	n/a	n/a	n/a	n/a	n/a	n/a
NiO	0.11	0.07	0.06	0.08	0.11	0.11	0.06	0.02	0.06	0.17	0.08	0.11	0.17	0.10	0.05	0.07	0.10
Total	99.94	99.60	100.11	99.88	99.51	99.51	99.55	99.01	99.48	99.01	99.17	99.59	99.36	99.12	99.07	99.10	99.67
Position		core	core	core		rim	rim	core	core	core		core	rim	core	core		rim
Oxygens		4	4	4	4	4	4	4	4	4	4	4	4	4	4	4	4
Si <sup>4+</sup>	0.002	0.000	0.001	0.001	0.001	0.001	0.001	0.001	0.001	0.001	0.001	0.002	0.003	0.001	0.000	0.001	0.001
Ti <sup>4+</sup>	--	0.001	0.001	--	--	0.002	0.001	0.001	--	--	--	0.002	0.026	--	--	--	0.016
Al <sup>3+</sup>	0.530	0.538	0.535	0.534	0.508	0.508	0.543	0.551	0.548	0.537	0.545	0.529	0.445	0.517	0.522	0.519	0.476
Cr <sup>3+</sup>	1.438	1.443	1.445	1.442	1.435	1.435	1.433	1.426	1.432	1.430	1.429	1.441	1.447	1.449	1.445	1.447	1.444
Fe <sup>2+</sup>	0.346	0.340	0.341	0.343	0.384	0.384	0.351	0.345	0.353	0.349	0.349	0.352	0.419	0.392	0.398	0.395	0.426
Mn <sup>2+</sup>	0.003	0.003	0.002	0.002	--	--	0.003	--	0.004	0.004	0.003	0.003	0.003	0.003	0.006	0.004	0.005
Mg <sup>2+</sup>	0.690	0.681	0.682	0.684	0.689	0.689	0.677	0.684	0.668	0.686	0.679	0.682	0.678	0.652	0.640	0.646	0.652
Ca <sup>2+</sup>	--	--	--	--	0.002	0.002	--	--	--	0.003	0.001	--	0.001	--	--	--	--
Na <sup>+</sup>	n/a	n/a	n/a	n/a	n/a	n/a	n/a	n/a	n/a	n/a	n/a	n/a	n/a	n/a	n/a	n/a	n/a
K <sup>+</sup>	n/a	n/a	n/a	n/a	n/a	n/a	n/a	n/a	n/a	n/a	n/a	n/a	n/a	n/a	n/a	n/a	n/a
Ni <sup>2+</sup>	0.003	0.002	0.002	0.002	0.003	0.003	0.001	0.001	0.002	0.004	0.002	0.003	0.004	0.003	0.001	0.002	0.003
Total	3.013	3.008	3.008	3.010	3.025	3.025	3.010	3.009	3.009	3.015	3.011	3.012	3.026	3.016	3.015	3.016	3.023

Table 6 Composition of minerals in sample 89487

Mineral	Olivine						Orthopyroxene						Clinopyroxene		
	87-1	87-2	87-5	87-15	87-11	87-12	87-13	87-14	Avg	87-5	87-6	87-6	87-6	87-6	87-6
Circle	1	1	3	7	6	6	6	6	6	3	3	3	3	3	3
SiO <sub>2</sub>	41.07	41.59	41.06	41.19	40.99	41.42	41.07	41.29	41.19	41.22	56.93	53.82			
TiO <sub>2</sub>	--	--	--	--	--	--	--	--	--	--	--	--	--	--	--
Al <sub>2</sub> O <sub>3</sub>	--	--	--	--	--	--	--	--	--	--	1.71	1.89			
Cr <sub>2</sub> O <sub>3</sub>	--	--	--	--	--	--	--	--	--	--	0.41	0.98			
FeO	7.20	7.22	7.29	7.51	7.74	7.64	7.62	7.47	7.62	7.37	5.06	1.54			
MnO	0.06	0.05	0.05	0.15	0.11	0.10	0.09	0.11	0.10	0.08	0.12	0.08			
MgO	50.73	50.86	50.96	50.57	50.86	51.06	50.95	50.93	50.95	50.81	34.74	17.30			
CaO	--	--	--	--	--	--	--	--	--	--	0.45	22.86			
Na <sub>2</sub> O	--	--	--	--	--	--	--	--	--	--	--	0.58			
K <sub>2</sub> O	n/a	n/a	n/a	n/a	n/a	n/a	n/a	n/a	n/a	n/a	--	--			
NiO	0.36	0.37	0.36	0.35	0.38	0.35	0.39	0.39	0.38	0.37	n/a	n/a			
Total	99.49	100.18	99.77	99.79	100.17	100.62	100.12	100.28	100.30	99.91	99.47	99.05			
Oxygens	4	4	4	4	4	4	4	4	4	4	6	6			
Si <sup>4+</sup>	1.000	1.000	1.000	1.000	1.000	1.000	1.000	1.000	1.000	1.000	1.963	1.965			
Ti <sup>4+</sup>	--	--	--	--	--	--	--	--	--	--	--	--	--	--	--
Al <sup>3+</sup>	--	--	--	--	--	--	--	--	--	--	0.069	0.081			
Cr <sup>3+</sup>	--	--	--	--	--	--	--	--	--	--	0.011	0.028			
Fe <sup>2+</sup>	0.147	0.145	0.148	0.152	0.158	0.154	0.155	0.151	0.155	0.149	0.146	0.047			
Mn <sup>2+</sup>	0.001	0.001	0.001	0.003	0.002	0.002	0.002	0.002	0.002	0.002	0.004	0.002			
Mg <sup>2+</sup>	1.841	1.823	1.850	1.830	1.849	1.838	1.849	1.838	1.844	1.837	1.785	0.941			
Ca <sup>2+</sup>	--	--	--	--	--	--	--	--	--	--	0.017	0.894			
Na <sup>+</sup>	--	--	--	--	--	--	--	--	--	--	--	0.041			
K <sup>+</sup>	n/a	n/a	n/a	n/a	n/a	n/a	n/a	n/a	n/a	n/a	--	--	--	--	--
Ni <sup>2+</sup>	0.007	0.007	0.007	0.007	0.008	0.007	0.008	0.008	0.007	0.007	n/a	n/a			
Total	2.998	2.979	3.008	2.993	3.019	3.002	3.014	3.002	3.009	2.997	3.998	4.001			
Mg#	0.93	0.93	0.93	0.92	0.92	0.92	0.92	0.92	0.92	0.92	0.92	0.95			

Table 6 continued

Mineral	Spinel									
Label	87-2	87-3	87-4	87-5	87-6	87-7	87-11	87-16	87-17	87-18
Circle	1	1	1	2	2	2	4	7a	7a	7b
SiO <sub>2</sub>	--	--	0.48	--	--	--	0.43	--	--	--
TiO <sub>2</sub>	--	--	--	--	--	--	--	--	--	--
Al <sub>2</sub> O <sub>3</sub>	25.04	25.43	24.93	24.82	24.45	23.22	22.97	26.74	20.53	24.20
Cr <sub>2</sub> O <sub>3</sub>	45.36	44.93	44.76	46.01	45.64	46.43	45.82	43.51	50.73	46.28
FeO	14.47	15.53	13.90	15.53	14.89	15.38	15.45	13.22	13.66	14.53
MnO	0.11	0.12	0.08	0.13	0.15	0.13	0.20	0.10	--	0.09
MgO	14.28	13.31	14.86	13.64	13.85	13.78	14.00	15.56	14.66	13.90
CaO	--	--	--	--	0.07	0.11	0.11	0.09	0.08	0.11
Na <sub>2</sub> O	n/a	n/a	n/a	n/a	n/a	n/a	n/a	n/a	n/a	n/a
K <sub>2</sub> O	n/a	n/a	n/a	n/a	n/a	n/a	n/a	n/a	n/a	n/a
NiO	--	--	0.09	--	--	--	0.13	--	0.09	--
Total	99.29	99.48	99.15	100.13	99.12	99.07	99.11	99.33	99.84	99.22
Position	core	core	rim	rim	core	rim	rim	core	rim	rim
Oxygens	4	4	4	4	4	4	4	4	4	4
Si <sup>4+</sup>	--	--	0.015	--	--	--	0.013	--	--	--
Ti <sup>4+</sup>	--	--	--	--	--	--	--	--	--	--
Al <sup>3+</sup>	0.897	0.913	0.890	0.887	0.882	0.844	0.833	0.944	0.745	0.872
Cr <sup>3+</sup>	1.090	1.081	1.072	1.103	1.104	1.132	1.115	1.031	1.234	1.119
Fe <sup>2+</sup>	0.368	0.396	0.352	0.394	0.381	0.397	0.398	0.331	0.352	0.372
Mn <sup>2+</sup>	0.003	0.003	0.002	0.003	0.004	0.003	0.005	0.002	--	0.002
Mg <sup>2+</sup>	0.647	0.604	0.671	0.617	0.632	0.633	0.642	0.695	0.672	0.634
Ca <sup>2+</sup>	--	--	--	--	0.002	0.004	0.004	0.003	0.003	0.004
Na <sup>+</sup>	n/a	n/a	n/a	n/a	n/a	n/a	n/a	n/a	n/a	n/a
K <sup>+</sup>	n/a	n/a	n/a	n/a	n/a	n/a	n/a	n/a	n/a	n/a
Ni <sup>2+</sup>	--	--	0.002	--	--	--	0.003	--	0.002	--
Total	3.006	3.001	3.004	3.005	3.006	3.012	3.013	3.010	3.009	3.004
Mg#	0.64	0.60	0.66	0.61	0.62	0.61	0.62	0.68	0.66	0.63